PACIFIC EARTHQUAKE ENGINEERING
RESEARCH CENTER

Response Spectrum Analysis of Concrete Gravity Dams Including Dam-Water-Foundation Interaction

Arnkjell Løkke
Department of Structural Engineering
Norwegian University of Science and Technology (NTNU)

Anil K. Chopra
Department of Civil and Environmental Engineering
University of California, Berkeley

PEER 2013/17
JULY 2013

Response Spectrum Analysis of Concrete Gravity Dams Including Dam-Water-Foundation Interaction

Arnkjell Løkke
Department of Structural Engineering
Norwegian University of Science and Technology (NTNU)

Anil K. Chopra
Department of Civil and Environmental Engineering
University of California, Berkeley

PEER Report 2013/17
Pacific Earthquake Engineering Research Center
Headquarters at the University of California, Berkeley

July 2013

ABSTRACT

A response spectrum analysis (RSA) procedure, which estimates the peak response directly from the earthquake design spectrum, was developed in 1986 for the preliminary phase of design and safety evaluation of concrete gravity dams. The analysis procedure includes the effects of dam-water-foundation interaction, known to be important in the earthquake response of dams.

This report presents a comprehensive evaluation of the accuracy of the RSA procedure by comparing its results with those obtained from response history analysis (RHA) of the dam modeled as a finite element system, including dam-water-foundation interaction. The earthquake response of an actual dam to an ensemble of 58 ground motions, selected and scaled to be consistent with a target spectrum determined from a probabilistic seismic hazard analysis for the dam site, was determined by the RHA procedure. The median of the peak responses of the dam to 58 ground motions provided the benchmark result. The peak response was also estimated by the RSA procedure directly from the median response spectrum. Comparison of the two sets of results demonstrated that the RSA procedure estimates stresses to a degree of accuracy that is satisfactory for the preliminary phase in the design of new dams and in the safety evaluation of existing dams. The accuracy achieved in the RSA procedure is noteworthy, especially considering the complicated effects of dam-water-foundation interaction and reservoir bottom absorption on the dynamics of the system, and the number of approximations necessary to develop the procedure.

Also developed in the report is a more complete set of data for the parameters that characterize dam-foundation interaction in the RSA procedure. Availability of these data should provide sufficient control over the overall damping in the dam-water-foundation system to ensure consistency with damping measured from motions of dams recorded during forced vibration tests and earthquakes.

ACKNOWLEDGMENTS

We are grateful to several individuals who helped in this research:

- Professor Gautam Dasgupta at Columbia University provided the computer program to compute new compliance data for a viscoelastic half-plane.
- Professor Baris Binici at the Middle East Technical University (METU) provided a set of Matlab scripts that were used as the starting point to develop pre- and post-processors to the EAGD-84 computer program, which was utilized to perform all the response history analyses presented in this report.
- Professor Pierre Léger at École Polytechnique de Montréal incorporated the new data presented in this report into the "pseudo-dynamic procedure" in the widely used computer program CADAM.

The first author would like to thank the Norwegian National Committee on Large Dams (NNCOLD) and Norwegian Water for their financial support during his visit to the University of California, Berkeley, in 2013 when this report was prepared.

The publication of this report by the Pacific Earthquake Engineering Research Center (PEER) is gratefully acknowledged. Any opinions, findings, and conclusions or recommendations expressed in this material are those of the authors and do not necessarily reflect those of PEER or any other sponsors.

TABLE OF CONTENTS

LIST OF FIGURES

LIST OF TABLES

1 Introduction

The elastic analysis phase of seismic design and safety evaluation of concrete gravity dams may be organized in two stages [Chopra 1978]: (1) response spectrum analysis (RSA) in which the peak value, i.e., the maximum absolute value, of response is estimated directly from the earthquake design spectrum; and (2) response history analysis (RHA) of a finite element idealization of the dam monolith. The RSA procedure was recommended for the preliminary phase of design and safety evaluation of dams, and the RHA procedure for accurately computing the dynamic response and checking the adequacy of the preliminary evaluation. Dam-water interaction effects were included in both procedures [Chopra 1978, Chakrabarti and Chopra 1973].

In the mid 1980s, both procedures were extended to consider absorption of hydrodynamic pressure waves into the alluvium and sediments invariably deposited at the bottom of reservoirs and, more importantly, interaction between the dam and underlying foundation [Fenves and Chopra 1984b, 1987]. Recognizing that the cross-sectional geometry of concrete gravity dams does not vary widely, standard data for the vibration properties of dams and parameters characterizing dam-water-foundation interaction effects were presented to facilitate the implementation of the RSA procedure [Fenves and Chopra 1987]. Both the RSA procedure, implemented in CADAM [Leclerc, Legér, and Tinawi 2003], and the RHA procedure, implemented in the computer program EAGD–84 [Fenves and Chopra 1984c], have been utilized extensively in seismic design of new dams and seismic evaluation of existing dams.

This report presents a comprehensive evaluation of the accuracy of the RSA procedure, in contrast to the limited scope of the earlier investigation [Fenves and Chopra 1987]. To enhance the accuracy of this RSA procedure, the possibility of calculating stresses by finite element analysis versus the commonly used beam formulas is explored, and a correction factor for beam stresses on the downstream face of the dam is developed. Also included is a more complete set of data for the parameters that characterize dam-foundation interaction. This was motivated by the realization that viscous damping of 5%, commonly assumed for rock, may be excessive, and that data presented earlier did not provide sufficient control over the overall damping in the dam-water-foundation system to ensure consistency with damping measured from motions of dams recorded during forced vibration tests and earthquakes [Rea, Liaw, and Chopra 1975; Proulx et. al. 2001; Alves and Hall 2006]. For the sake of completeness, the RSA procedure is summarized

and standard values for parameters that characterize dam-water interaction and reservoir bottom absorption are included, thus making this report self-contained.

2 Response Spectrum Analysis Procedure

The response spectrum analysis (RSA) procedure developed to estimate the earthquake-induced stresses in concrete gravity dams considers only the more significant aspects of the response. Although the dynamics of the system including dam-water-foundation interaction is considered in estimating the response due to the fundamental vibration mode, the less significant part of the response due to higher modes is estimated by the static correction method. Only the horizontal component of ground motion is considered because the response due to the vertical component is known to be much smaller [Fenves and Chopra 1984a].

Dam-water-foundation interaction introduces frequency-dependent, complex-valued hydrodynamic and foundation terms in the governing equations. Based on a clever series of approximations, frequency-independent values of these terms were defined and an equivalent SDF system developed to estimate the fundamental mode response of dams, leading to the RSA procedure summarized in the subsequent sections. This development was presented and approximations evaluated and justified in a series of publications [Fenves and Chopra 1985a, 1985b, 1987].

The two-dimensional system considered consists of a concrete gravity dam monolith supported on a horizontal surface of underlying flexible foundation rock idealized as a viscoelastic half-plane, and impounding a reservoir of water, possibly with alluvium and sediments at the bottom (Figure 2.1). A complete description of the dam-water-foundation system is presented in Fenves and Chopra [1984b, 1985a].

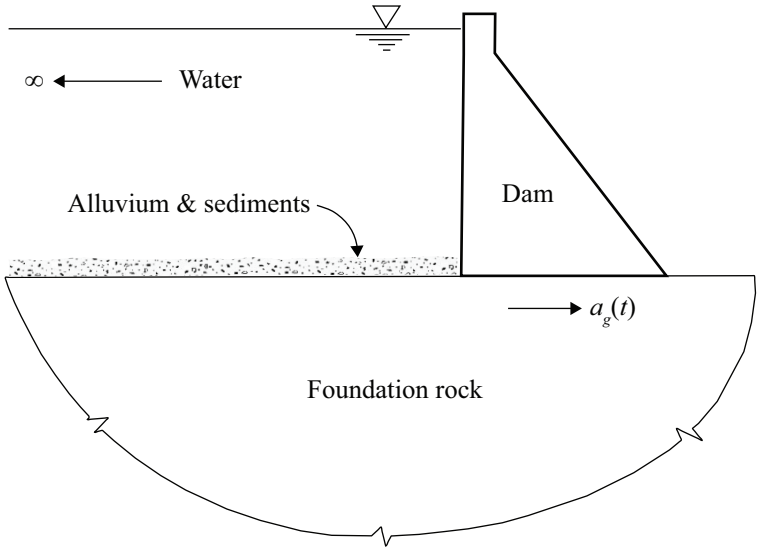

Figure 2.1 Dam-water-foundation system.

2.1 EQUIVALENT STATIC LATERAL FORCES: FUNDAMENTAL MODE

The peak response of the dam in its fundamental vibration mode including dam-water-foundation interaction effects can be estimated by static analysis of the dam alone subjected to equivalent static lateral forces acting on the upstream face of the dam:

$$f_1(y) = \tilde{\Gamma}_1 \frac{A\left(\tilde{T}_1, \tilde{\zeta}_1\right)}{g}\left[w_s(y)\phi_1(y) + gp\left(y, \tilde{T}_r\right)\right] \tag{2.1}$$

in which $\phi_1(y)$ is the horizontal component of displacement at the upstream face of the dam in the fundamental vibration mode shape of the dam supported on rigid foundation with empty reservoir; $w_s(y)$ is the weight per unit height of the dam; and $\tilde{\Gamma}_1 = \tilde{L}_1 / \tilde{M}_1$, where $\tilde{M}_1$ and $\tilde{L}_1$ are given by

$$\tilde{M}_1 = M_1 + \int_0^H p\left(y, \tilde{T}_r\right)\phi_1(y)\,dy \tag{2.2}$$

$$\tilde{L}_1 = L_1 + \int_0^H p\left(y, \tilde{T}_r\right)dy \tag{2.3}$$

in which H is the depth of the impounded water; the generalized mass and earthquake force coefficient are given by

$$M_1 = \frac{1}{g}\int_0^{H_s} w_s(y)\phi_1^2(y)\,dy \tag{2.4}$$

$$L_1 = \frac{1}{g}\int_0^{H_s} w_s(y)\phi_1(y)\,dy \tag{2.5}$$

where H_s is the height of the dam; g is the acceleration due to gravity; and $A(\tilde{T}_1, \tilde{\zeta}_1)$ is the pseudo-acceleration ordinate of the earthquake design spectrum evaluated at vibration period $\tilde{T}_1$ and damping ratio $\tilde{\zeta}_1$ of the equivalent SDF system representing the dam-water-foundation system.

The function $p(y, \tilde{T}_r)$ is the real-valued component of the complex-valued function representing the hydrodynamic pressure on the upstream face due to harmonic acceleration at period $\tilde{T}_r$ in the shape of the fundamental mode; the corresponding boundary value problem is shown in Figure 2.2a. The natural vibration period of the equivalent SDF system representing the fundamental mode response of the dam (on rigid foundation) with impounded water is given by [Fenves and Chopra 1985a]

$$\tilde{T}_r = R_r T_1 \tag{2.6}$$

in which T_1 is the fundamental vibration period of the dam on rigid foundation with empty reservoir. Hydrodynamic effects lengthen the vibration period, i.e., the period-lengthening ratio, R_r, is greater than one because of the frequency-dependent, added hydrodynamic mass arising from dam-water interaction. It depends on the properties of the dam, the depth of the water, and the absorptiveness of the reservoir bottom materials.

The natural vibration period of the equivalent SDF system representing the fundamental mode response of the dam (with empty reservoir) on flexible foundation is given by [Fenves and Chopra 1985a]

$$\tilde{T}_f = R_f T_1 \tag{2.7}$$

Dam-foundation interaction lengthens the vibration period, i.e., the period-lengthening ratio, R_f, is greater than one because of the frequency-dependent, added foundation flexibility arising from dam-foundation interaction. It depends on the properties of the dam and foundation, most importantly, on the ratio E_f / E_s of the elastic moduli of the foundation and the dam concrete.

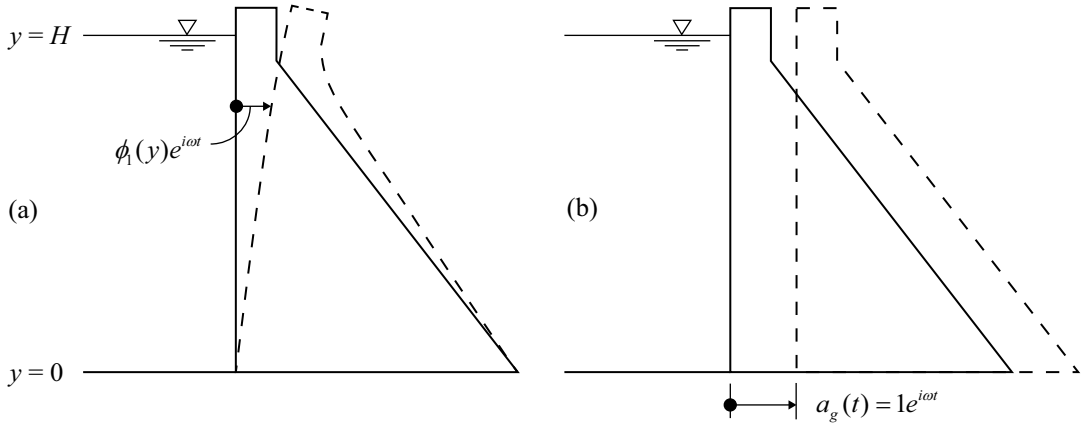

Figure 2.2 **(a) Acceleration of a dam in its fundamental mode shape; (b) horizontal acceleration of a rigid dam.**

The natural vibration period of the equivalent SDF system representing the fundamental mode response of the dam including dam-water-foundation interaction is given by [Fenves and Chopra 1985b]

$$\tilde{T}_1 = R_r R_f T_1 \tag{2.8}$$

The damping ratio of this equivalent SDF system can be expressed as [Fenves and Chopra 1985b]

$$\tilde{\zeta}_1 = \frac{1}{R_r}\frac{1}{(R_f)^3}\zeta_1 + \zeta_r + \zeta_f \tag{2.9}$$

in which ζ_1 is the damping ratio of the dam on rigid foundation with empty reservoir; ζ_r is the added damping due to dam-water interaction and reservoir bottom absorption; and ζ_f is the added radiation and material damping due to dam-foundation interaction. Considering that $R_r > 1$ and $R_f > 1$, Equation (2.9) shows that dam-water interaction and dam-foundation interaction reduce the effectiveness of structural (dam) damping. However, usually this reduction is more than compensated by (a) added damping due to reservoir bottom absorption and (b) dam-foundation interaction, which leads to an increase in the overall damping of the dam.

Before closing this section, we note that the equivalent static lateral forces $f_1(x,y)$ vary over the cross section of the dam monolith. These were integrated over the breadth of the monolith to obtain the forces per unit height of the dam, see Equation (2.1). The variation of the fundamental mode shape $\phi_1^x(x,y)$ over the breadth of the dam is thus neglected, i.e., $\phi_1^x(x,y) \approx \phi_1^x(0,y)$, and the fundamental mode shape at the upstream face of the dam, $\phi_1(y) \equiv \phi_1^x(0,y)$, is used in all subsequent calculations. The implication of the one-dimensional formulation of lateral forces to the estimation of stresses is discussed in Chapter 6.

2.2 EQUIVALENT STATIC LATERAL FORCES: HIGHER MODES

Although the fundamental vibration mode is dominant in the response of the dam, the contributions of the higher modes are included by approximating them using the "static correction" concept [Chopra 2012: Section 12.12 and 13.1.5]. This implies that the ordinates of the pseudo-acceleration design spectrum at the higher mode periods are approximated by the zero-period ordinate, i.e., the peak ground acceleration. The quality of this approximation depends on dynamic amplification of the design spectrum at the higher mode periods, as will be discussed in Chapter 6.

Just as in the case of multistory buildings [Veletsos 1977], soil-structure (dam-foundation) interaction effects may be neglected in a simplified procedure to compute the contributions of the higher vibration modes to the earthquake response of dams.

Utilizing the preceding concepts, the equivalent lateral earthquake forces associated with the higher vibration modes of dams, including the effects of the impounded water, are given by [Fenves and Chopra 1987]

$$f_{\mathrm{sc}}(y)=\frac{a_g}{g}\left\{w_s(y)\left[1-\frac{L_1}{M_1}\phi_1(y)\right]+\left[gp_0(y)-\frac{B_1}{M_1}w_s(y)\phi_1(y)\right]\right\} \tag{2.10}$$

In Equation (2.10), a_g is the peak ground acceleration; $p_0(y)$ is a real-valued frequency-independent function for hydrodynamic pressure on a rigid dam undergoing unit acceleration, with water compressibility neglected (Figure 2.2b) (both assumptions being consistent with the "static correction" concept); and B_1 provides a measure of the portion of $p_0(y)$ that acts in the fundamental vibration mode:

$$B_1=0.20\frac{F_{\mathrm{st}}}{g}\left(\frac{H}{H_s}\right)^2 \tag{2.11}$$

where F_{st} is the total hydrostatic force on the dam. The shape of only the fundamental vibration mode enters into Equation (2.10) and the higher mode shapes are not required, thus simplifying the analysis considerably.

2.3 RESPONSE ANALYSIS

As shown in the preceding two sections, the maximum effects of earthquake ground motion in the fundamental vibration mode of the dam have been represented by equivalent static lateral forces $f_1(y)$ and those due to all the higher modes by $f_{\mathrm{sc}}(y)$, determined directly from the response (or design) spectrum without any response history analyses. Static analysis of the dam alone for these two sets of forces provide estimates of the peak modal responses r_1 and r_{sc} for

any response quantity, r, e.g., the shear force or bending moment at any horizontal section, or the shear stress or vertical stress at any point. The total response is given by

$$r_{\max} = r_{\text{st}} \pm \sqrt{\left(r_{\text{I}}\right)^2 + \left(r_{\text{sc}}\right)^2} \tag{2.12}$$

where the initial value, r_{st}, of the response quantity prior to the earthquake is determined by standard static analysis procedures, including the effects of the self-weight of the dam, hydrostatic pressures, construction sequence, and thermal effects.

In Equation (2.12) the dynamic response is obtained by combining peak modal responses r_{I} and r_{sc} in the fundamental and higher modes, respectively, by the SRSS rule, which is appropriate because the natural vibration frequencies of a concrete gravity dam are well separated. Because the directions of earthquake responses are reversible, both positive and negative signs are included in the dynamic response.

The SRSS combination rule is applicable to the computation of any response quantity that is proportional to the modal coordinates [Chopra 2012: Section 13.8]. Thus, this rule is generally not valid to determine the principal stresses. However, the maximum principal stresses at the two faces of the dam can be determined by a simple transformation of the vertical stresses—determined by beam theory—if the upstream face is nearly vertical and the effects of tail-water at the downstream face are small [Fenves and Chopra 1986: Appendix C]. Under these restricted conditions, the resulting principal stresses at the two faces of a dam monolith (*not in the interior*) may be determined by the SRSS rule.

The preceding combination of static and dynamic responses is appropriate if r_{st}, r_{I}, and r_{sc} are oriented similarly. Such is obviously the case for the shear and vertical stresses at any point, but generally not for principal stresses except under the restricted conditions previously mentioned.

3 Standard System Properties for Fundamental Mode Response

The computations required to directly evaluate Equation (2.1) would be excessive in practical application. Recognizing that the cross-sectional geometry of concrete gravity dams does not vary widely, standard values for the vibration properties—vibration period and shape of the fundamental mode—of the dam, period lengthening ratios R_r and R_f due to dam-water and dam-foundation interaction, damping ratios ζ_r and ζ_f associated with the two interaction mechanisms, and the hydrodynamic pressure functions $p(y,\tilde{T}_r)$ and $p_0(y)$ are presented in this chapter. They represent an extension of the data first presented in Fenves and Chopra [1986].

3.1 VIBRATION PROPERTIES FOR THE DAM

The fundamental vibration period, in seconds, for a "standard" cross section (Figure 3.1a) for non-overflow monoliths of concrete gravity dams on rigid foundation with an empty reservoir can be approximated by [Chopra 1978]

$$T_1 = 1.4\frac{H_s}{\sqrt{E_s}} \tag{3.1}$$

where H_s is the height of the dam in feet, and E_s is the modulus of elasticity of the dam concrete in psi. The fundamental vibration mode shape, $\phi_1(y)$, of the "standard" cross section is shown in Figure 3.1b and presented in Table A.1. These standard vibration properties are compared in Figure 3.1b with the fundamental vibration periods and mode shapes determined by finite element analyses of six cross sections—two actual dams and four idealized dams—chosen to cover the plausible range of shapes. This comparison demonstrates that it is appropriate to use the standard vibration period and mode shape for preliminary design and safety evaluation of concrete gravity dams.

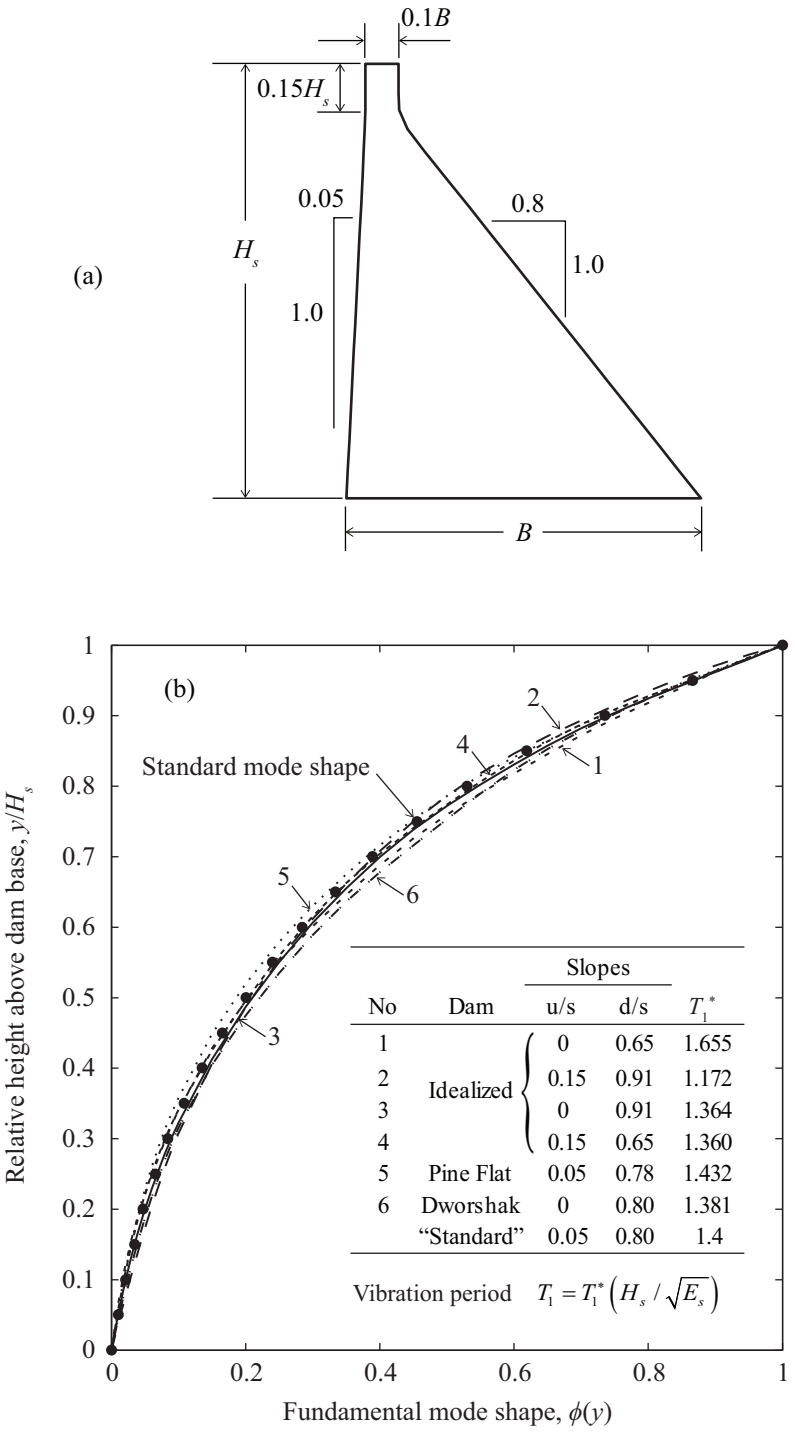

Figure 3.1 **(a) "Standard" cross-section; (b) comparison of fundamental vibration period and mode shape for the "standard" cross-section and four idealized and two actual concrete gravity dam cross-sections. Data from Chopra [1978].**

3.2 MODIFICATION OF PERIOD AND DAMPING DUE TO DAM-WATER INTERACTION

Dam-water interaction and reservoir bottom absorption modify the natural vibration period and damping ratio of the equivalent SDF system. For the "standard" dam cross section, the period lengthening ratio R_r and added damping ζ_r are dependent on several parameters, the most significant being: modulus of elasticity E_s of the dam concrete, the ratio H/H_s of water depth to dam height, and the wave reflection coefficient α. This coefficient, α, is the ratio of the amplitude of the reflected hydrodynamic pressure wave to the amplitude of a vertically propagating pressure wave incident on the reservoir bottom [Fenves and Chopra 1983, 1984b], where $\alpha = 1$ indicates complete reflection of pressure waves, and smaller values of α indicate increasingly absorptive materials.

By performing many analyses of the "standard" dam cross section using the procedures described in Fenves and Chopra (1984a) and modified in Appendix A of Fenves and Chopra (1986) for dams with large values of modulus of elasticity E_s, period lengthening ratio R_r and added damping ratio ζ_r have been computed as a function of H/H_s for a range of values of E_s and α [Fenves and Chopra 1986]; results are summarized in Table A.2.

The mechanics of dam-water interaction and reservoir bottom absorption has been discussed elsewhere in detail [Fenves and Chopra 1983, 1984b]. Here, we simply note that R_r increases and ζ_r generally—but not always—increases, with increasing water depth, absorptiveness of the reservoir bottom materials, and elastic modulus of concrete. The effects of dam-water interaction may be neglected in the analysis if the reservoir depth is less than half of the dam height, i.e., $H/H_s < 0.5$.

3.3 MODIFICATION OF PERIOD AND DAMPING DUE TO DAM-FOUNDATION INTERACTION

Dam-foundation interaction modifies the natural vibration period and damping ratio of the equivalent SDF system. For the "standard" dam cross section, period lengthening ratio R_f and added damping ζ_f depend on several parameters, the most significant being: E_f/E_s, the ratio of the moduli of elasticity of the foundation rock to that of the dam concrete; and η_f, the constant hysteretic damping factor for the foundation rock.

By performing many analyses of the "standard" dam cross section using the procedures described in Fenves and Chopra [1984a], period lengthening ratio R_f and added damping ratio ζ_f were initially computed for a range of values of E_f/E_s and η_f = 0.01, 0.10, 0.25, and 0.50 [Fenves and Chopra 1986], which in retrospect turned out to be too coarse. The added damping ratio has now been recomputed for a closely spaced set of η_f values; the results are presented in Table A.3.

The mechanics of dam-foundation interaction has been discussed elsewhere in detail [Fenves and Chopra 1984b]. Here we simply note that for moduli ratios E_f/E_s that are representative of actual dam sites, the period ratio R_f varies little with η_f; therefore a single curve represents the variation of R_f with E_f/E_s, which may be used for any value of η_f. As expected, R_f increases as the moduli ratio E_f/E_s decreases, which for a fixed value of E_s implies that the foundation is increasingly flexible. The added damping ratio ζ_f increases with decreasing E_f/E_s and increasing constant hysteretic damping factor η_f. The foundation may be treated as rigid in the analysis if $E_f/E_s > 4$, as the effects of dam-foundation interaction are then negligible.

3.4 HYDRODYNAMIC PRESSURE

In order to provide a convenient means for determining the hydrodynamic pressure function $p(y,\tilde{T}_r)$ in Equation (2.1), a non-dimensional form of this function, $gp(\hat{y})/wH$, where $\hat{y} = y/H$ and w is the unit weight of water, was computed in Fenves and Chopra (1986) for several values of α and a range of the period ratio

$$R_w = \frac{T_1^r}{\tilde{T}_r} \tag{3.2}$$

where T_1^r is the fundamental vibration period of the impounded water given by $T_1^r = 4H/C$, where C is the velocity of pressure waves in the water. Results for a full reservoir, $H/H_s = 1$, and a range of values of α and R_w are summarized in Table A.4. The function $gp(\hat{y})/wH$ for other values of H/H_s can be approximately computed as $(H/H_s)^2$ times the function for $H/H_s = 1$ [Chopra 1978].

3.5 GENERALIZED MASS AND EARTHQUAKE FORCE COEFFICIENT

Instead of evaluating Equations (2.2) and (2.3), the generalized mass, $\tilde{M}_1$, and generalized earthquake coefficient, $\tilde{L}_1$, of the equivalent SDF system including hydrodynamic effects can be conveniently computed from [Fenves and Chopra 1986]

$$\tilde{M}_1 = (R_r)^2 M_1 \tag{3.3}$$

$$\tilde{L}_1 = L_1 + \frac{1}{g} F_{\text{st}} \left(\frac{H}{H_s} \right)^2 A_p \tag{3.4}$$

where $F_{\text{st}} = wH^2/2$ is the hydrostatic force, and the hydrodynamic force coefficient A_p is the integral over the depth of water of the pressure function $2gp(\hat{y})/wH$ for $H/H_s = 1$. The hydrodynamic force coefficient, A_p, computed in Fenves and Chopra [1986] for a range of values for period ratio R_w and wave reflection coefficient α, are summarized in Table A.5.

4 Implementation of Analysis Procedure

4.1 SELECTION OF SYSTEM PARAMETERS AND EARTHQUAKE DESIGN SPECTRUM

The response spectrum analysis (RSA) procedure requires only a few parameters to describe the dam-water-foundation system: E_s, ζ_1, H_s, E_f, η_f, H, and α. In addition, a pseudo-acceleration design spectrum is required to represent the seismic hazard at the site. Based on the recommendations presented in Fenves and Chopra [1987], with a few modifications, guidelines for selecting the system parameters to be used in the RSA procedure are presented in this section.

The Young's modulus of elasticity E_s for the dam concrete should be based on suitable test data—in so as far as possible—or estimated from the design strength of concrete. The value of E_s may be modified to recognize the strain rates representative of those the concrete may experience during earthquake motions of the dam [Chopra 1978]. The dam-water interaction parameters R_r and ζ_r may be estimated for the selected E_s value by linearly interpolating, if necessary, between the nearest values for which data are available in Table A.2: E_s = 1.0, 2.0, 2.5, 3.0, 3.5, 4.0, 4.5, or 5.0 million psi. Correlation of recorded and computed motions of dams during earthquakes [Chopra and Wang 2010], indicates that the viscous damping ratio ζ_1 for the dam alone is in the range of 1 to 3%. Assigning a value for ζ_1 in this range is recommended if no data specific to the dam is available. The height H_s of the dam is measured from the base to the crest.

The Young's modulus of elasticity E_f and constant hysteretic damping coefficient η_f of the foundation rock should be determined from a site investigation and appropriate tests. For the resulting value of E_f/E_s, the dam-foundation interaction parameters R_f and ζ_f can be estimated by linearly interpolating, if necessary, between the two nearest values for which data are available in Table A.3. In the absence of measured properties for the rock at the site, a value of η_f in the range of 0.02–0.06 is recommended [Chopra and Wang 2010], corresponding to a viscous damping ratio of 1–3%.

The depth H of the impounded water is measured from the free surface to the reservoir bottom. In practical situations the elevations of the reservoir bottom and dam base may differ. The standard values for unit weight of water and velocity of pressure waves in water are $w = 62.4$ pcf and $C = 4720$ ft/sec, respectively.

It may be impractical to determine reliably the wave reflection coefficient α because the reservoir bottom materials may consist of highly variable layers of exposed bedrock, alluvium, silt, and other sediments, and appropriate site investigation techniques have not been developed. However, to be conservative, the estimated value of α should be rounded up to the nearest value for which data are presented: α = 1.0, 0.90, 0.75, 0.50, 0.25, and 0; interpolation of data for intermediate values of α is not appropriate. For proposed new dams or recent dams where sediment deposits are meager, α = 0.90 or 1.0 is recommended and, lacking data, α = 0.75 or 0.90 is recommended for older dams where sediment deposits are substantial. In each case, the larger α value will generally give conservative results, which is appropriate at the preliminary design stage.

The horizontal earthquake ground acceleration is specified by a pseudo-acceleration design spectrum in the RSA procedure. This should be a smooth response spectrum—without the irregularities inherent in response spectra of individual ground motions—representative of the intensity and frequency characteristics of the earthquake events associated with the seismic hazard at the site.

4.2 COMPUTATIONAL STEPS

Computation of the earthquake response of the dam is organized in three parts [Fenves and Chopra 1987]:

Part I: Compute the earthquake forces and stresses due to response of the dam in its fundamental mode of vibration by the following computational steps:

l. Compute T_1, the fundamental vibration period of the dam, in seconds, on rigid foundation with an empty reservoir from Equation (3.1) in which H_s is the height of the dam in feet, and E_s is the design value of the modulus of elasticity of dam concrete in psi.

2. Compute $\tilde{T}_r$, the fundamental vibration period of the dam, in seconds, including the influence of impounded water from Equation (2.6) in which T_1 was computed in Step 1; R_r is the period ratio determined from Table A.2 for the design values of E_s, the wave reflection coefficient α, and the depth ratio H/H_s, where H is the depth of the impounded water. If $H/H_s < 0.5$, computation of R_r may be avoided by using $R_r = 1$.

3. Compute the period ratio R_w from Equation (3.2) in which $\tilde{T}_r$ was computed in Step 2; and $T_1^r = 4H/C$ where C = 4720 ft/sec.

4. Compute $\tilde{T}_1$, the fundamental vibration period of the dam, in seconds, including the dam-water-foundation interaction, from Equation (2.8) in which R_r was determined in Step 2; R_f is the period ratio determined from Table A.3 for the design value of E_f/E_s; and E_f is the modulus of elasticity of the foundation. If $E_f/E_s > 4$, use $R_f \approx 1$.

5. Compute the damping ratio $\tilde{\zeta}_1$ of the dam from Equation (2.9) using the computed period ratios R_r and R_f; ζ_1 is the viscous damping ratio for the dam on rigid foundation with empty reservoir; ζ_r is the added damping ratio due to dam-water interaction and reservoir bottom absorption, obtained from Table A.2 for the selected values of E_s, α and H/H_s; ζ_f is the added damping ratio due to dam-foundation interaction, obtained from Table A.3 for the selected values of E_f/E_s, and η_f. If $H/H_s < 0.5$, use $\zeta_r = 0$; if $E_f/E_s > 4$, use $\zeta_f = 0$; and if the computed value of $\tilde{\zeta}_1 < \zeta_1$, use $\tilde{\zeta}_1 = \zeta_1$.

6. Determine $gp(y, \tilde{T}_r)$ from Table A.4 corresponding to the value of R_w computed in Step 3 (by interpolating, if necessary, between data for the two nearest available values of R_w), the design value of α, and for $H/H_s = 1$; the result is multiplied by $(H/H_s)^2$. If $H/H_s < 0.5$, computation of $p(y, \tilde{T}_r)$ may be avoided by using $p(y, \tilde{T}_r) \approx 0$.

7. Compute the generalized mass, $\tilde{M}_1$, from Equation (3.3) in which R_r was computed in Step 2; and M_1 is computed from Equation (2.4) in which $w_s(y)$ is the weight of the dam per unit height; the fundamental vibration mode shape $\phi_1(y)$ is tabulated in Table A.1; and g is the acceleration due to gravity.

8. Compute the generalized earthquake force coefficient $\tilde{L}_1$ from Equation (3.4) in which L_1 is computed from Equation (2.5); $F_{st} = wH^2/2$; and A_p is given in Table A.5 for the values of R_w and α used in Step 6. If $H/H_s < 0.5$, computation of $\tilde{L}_1$ may be avoided by using $\tilde{L}_1 \approx L_1$.

9. Compute $f_1(y)$, the equivalent static lateral earthquake forces associated with the fundamental vibration mode from Equation (2.1) in which $A(\tilde{T}_1, \tilde{\zeta}_1)$ is the pseudo-acceleration ordinate of the earthquake design spectrum evaluated at the vibration period $\tilde{T}_1$ determined in Step 4 and damping ratio $\tilde{\zeta}_1$ determined in Step 5; $w_s(y)$ is the weight per unit height of the dam; $\phi_1(y)$ is the fundamental vibration mode shape of the dam from Table A.1; $\tilde{\Gamma}_1 = \tilde{L}_1/\tilde{M}_1$ where $\tilde{L}_1$ and $\tilde{M}_1$ was determined in Steps 7 and 8, respectively; and the hydrodynamic pressure term $gp(y, \tilde{T}_r)$ was determined in Step 6.

10. Determine by static analysis of the dam subjected to the equivalent static lateral forces $f_1(y)$, from Step 9, applied to the upstream face of the dam, all the response quantities of interest, in particular, the stresses throughout the dam. Traditional procedures for design calculations may be used wherein the bending stresses across a horizontal section are computed by elementary formulas for stresses in beams. Alternatively, the finite element method may be used for a more accurate static stress analysis.

    Note: If computed using beam theory, stresses at the sloping part of the downstream face should be multiplied by the correction factor of 0.75 developed in Section 4.3.

Part II: The earthquake forces and stresses due to the higher vibration modes can be determined approximately for purposes of preliminary design by the following computational steps:

11. Compute $f_{sc}(y)$, the equivalent static lateral earthquake forces associated with the higher vibration modes from Equation (2.10) in which M_1 and L_1 were determined in Steps 7 and 8, respectively; $gp_0(y)$ is determined from Table A.6; B_1 is computed from Equation (2.11); and a_g is the peak ground acceleration from the earthquake design spectrum. If $H/H_s < 0.5$, computation of $p_0(y)$ may be avoided by using $p_0(y) \approx 0$ and hence $B_1 \approx 0$.

12. Determine by static analysis of the dam subjected to the equivalent static lateral forces $f_{sc}(y)$, from Step 11, applied to the upstream face of the dam, all the response quantities of interest, in particular, the stresses throughout the dam. The stress analysis may be carried out by the same procedures mentioned in Step 10.

Part III: The total bending moments, shear forces and stresses at any section in the dam are determined by the following computational step:

13. Compute the total value of any response quantity from Equation (2.12) in which r_1 and r_{sc} are values of the response quantity determined in Steps 10 and 12 associated with the fundamental and higher vibration modes, respectively; and r_{st} is its initial value prior to the earthquake due to various loads, including the self-weight of the dam, hydrostatic pressure, construction sequence, and thermal effects.

4.3 CORRECTION FACTOR FOR DOWNSTREAM FACE STRESSES

Formulas based on beam theory overestimate stresses at sloping faces, thus, stresses computed at the downstream face of concrete gravity dams should be multiplied by the correction factor developed in this section.

Figure 4.1 shows the vertical stresses, $\sigma_{y,1}$, at the upstream and downstream faces of Pine Flat Dam (Figure 6.1), which is typical of many dams, with empty reservoir on rigid foundation, due to the lateral forces of Equation (2.1). Stresses were computed by static analysis using beam formulas and the finite element method; a detailed summary of the procedure is included in Appendix C. It is evident that beam theory provides results close to those from finite element analysis at the upstream face, but the stresses at the downstream face are considerably overestimated. Multiplying the stress values at the sloping part of the downstream face by a correction factor of 0.75 leads to stresses that are much closer to the finite element values. However, the agreement is not as good near the toe of the dam and at the stress concentration where the downstream face changes slope.

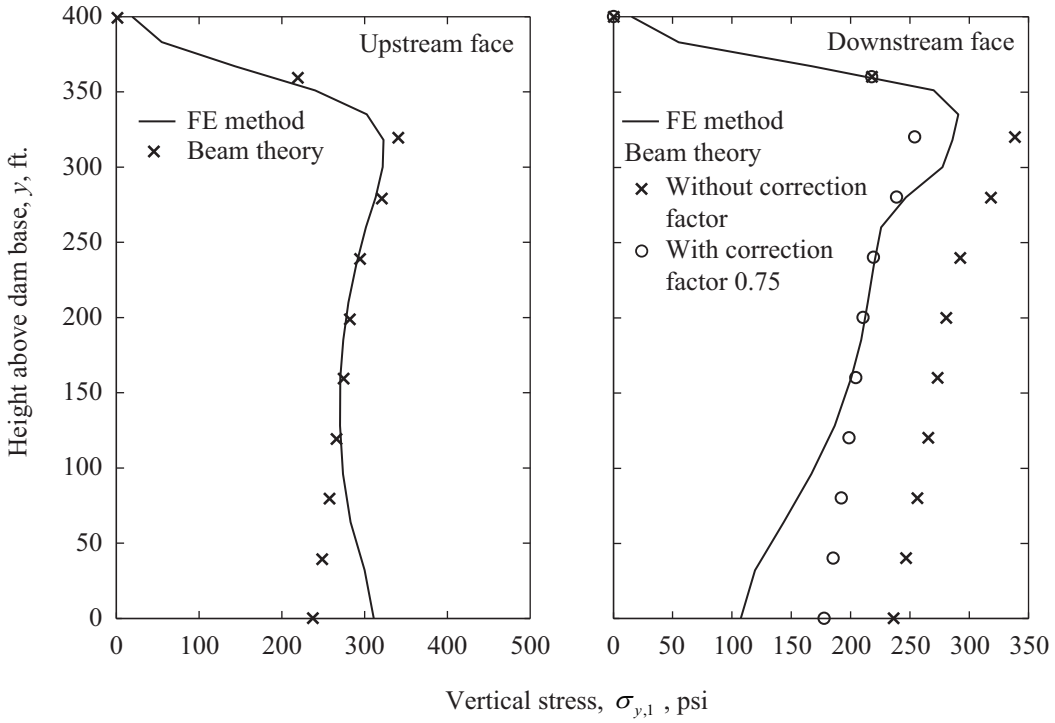

Figure 4.1 **Vertical stresses, $\sigma_{y,1}$, at the upstream and downstream face of Pine Flat Dam with empty reservoir on rigid foundation due to the lateral forces of Equation (2.1).**

The correction factor of 0.75 is applicable for modifying vertical stresses computed by beam theory if the slope of the downstream face is no steeper than 0.8:1; it will give conservative results for flatter slopes, but will underestimate the stresses if the slope is much steeper than 0.8:1. The same correction factor is applicable to the principal stresses computed by beam theory at the downstream face of the dam provided the stresses due to tail-water are negligible. With this restriction, the principal stresses are directly proportional to the vertical stresses [Fenves and Chopra 1986].

Although the correction factor was determined from computed stresses due to the lateral forces associated with the fundamental mode only, it may also be applied to the higher mode stresses, $\sigma_{y,\mathrm{sc}}$. The effectiveness of the correction factor applied to both modal contributions is demonstrated in Section 6.3.

4.4 USE OF S.I. UNITS

Because the standard values for most quantities required in the RSA procedure are presented in a non-dimensional form, implementation of the procedure using S.I. units is straightforward. The expressions and data requiring conversion to S.I. units are noted here:

1. The fundamental vibration period T_1 of the dam on rigid foundation with empty reservoir (Step l), in seconds, is given by:

$$T_1 = 0.38\frac{H_s}{\sqrt{E_s}} \tag{4.1}$$

where H_s is the height of the dam in meters; and E_s is the modulus of elasticity of the dam concrete in MPa.

2. The period ratio R_r and added damping ratio ζ_r due to dam-water interaction presented in Table A.2 is for specified values of E_s in psi, which should be converted to MPa as follows: 1 million psi $\approx$ 7 thousand MPa.

3. Where required in the calculations, the unit weight of water $w = 9.81\text{kN/m}^3$, the acceleration due to gravity $g = 9.81\text{m/s}^2$, and velocity of pressure waves in water $C = 1440\text{ m/sec}$.

5 CADAM Computer Program

CADAM—computer aided stability analysis of gravity dams—is a computer program, freely available, developed at the École Polytechnique de Montréal, Canada for static and seismic stability evaluations of concrete gravity dams [Leclerc, Legér and Tinawi 2003]. A screenshot of the user interface is shown in Figure 5.1. Based on the gravity method, CADAM uses rigid body equilibrium and beam theory to perform stress analyses and compute crack lengths and safety factors for dams subjected to various static and seismic load cases (listed in Figure 5.2); a summary of the analyses options available in the program is listed in Table 5.1.

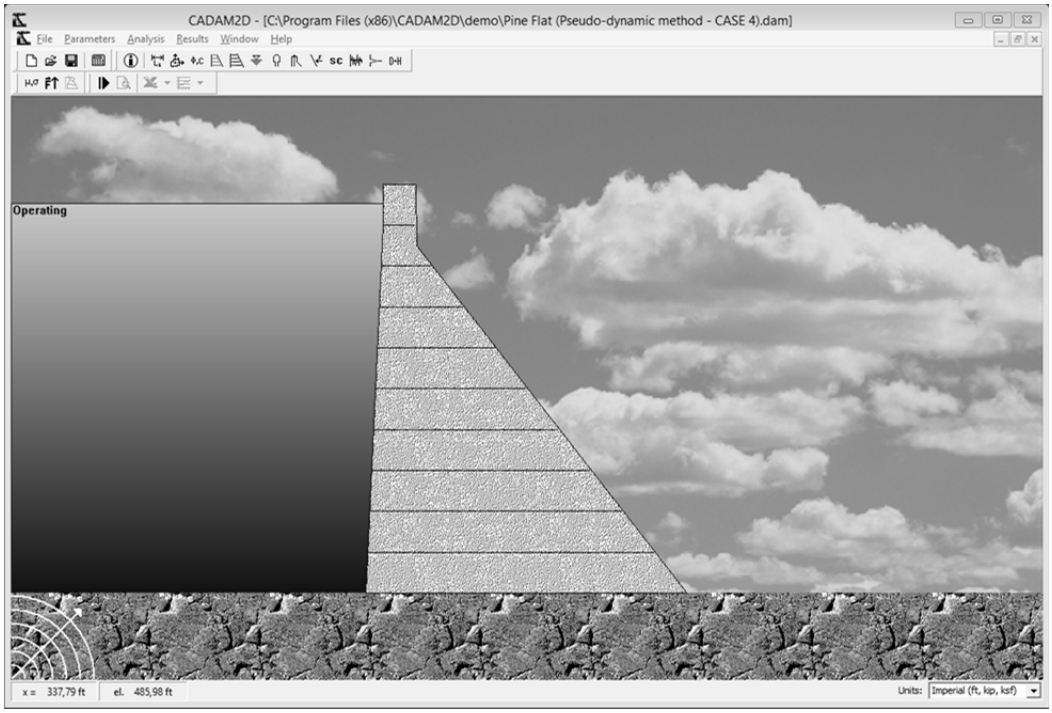

Figure 5.1 Screenshot of CADAM user interface.

Table 5.1 List of analysis options currently available in CADAM [Leclerc, Legér, and Tinawi 2002].

Static analyses	Static analyses are performed for the normal operating reservoir elevation or the flood elevation including overtopping over the crest and floating debris.
Seismic analyses	Seismic analyses are performed using the pseudo-static method (seismic coefficient method) or the pseudo-dynamic method.
Post-seismic analyses	In post-seismic safety analysis, the crack length induced by the seismic event could alter the cohesive shear resistance and uplift pressures. The post-seismic uplift pressures could either (a) build-up to its full value in seismic cracks or (b) return to its initial value if the seismic crack is closed after the earthquake.
Incremental load analyses	Sensitivity analyses are automatically performed by computing and plotting the evolution of typical performance indicators (ex: sliding safety factor) as a function of a progressive application in the applied loading (ex: reservoir elevation, peak ground acceleration).
Probabilistic safety analyses	Probabilistic safety analyses are performed to compute the probability of failure of a dam-foundation-reservoir system as a function of the uncertainties in loading and strength parameters that are considered as random variables with specified probability density functions. A Monte-Carlo simulation computational procedure is used. Static, seismic, as well as post-seismic analyses may be considered.

CADAM implements the RSA procedure, referring to it as the "pseudo-dynamic method." Starting with user input, the program computes the equivalent static lateral forces associated with the response of the system in its fundamental mode and higher vibration modes by implementing the procedure as described in Chapter 4 of this report. The earthquake-induced bending moments, shear forces, and stresses due to the two sets of forces are computed and combined to determine the total dynamic response. Finally, the responses due to earthquake forces and initial static loads can be combined.

The program provides a fully integrated computing environment with output reports and graphical support to visualize input parameters and output performance indicators such as stresses, crack lengths, resultant positions and safety factors. In addition, output can be exported to Microsoft Excel spreadsheets to allow users to perform further post-processing of results.

CADAM is widely used for educational purposes, R&D in dam engineering, and in actual projects. A complete description of the program and its capabilities can be found in Leclerc, Legér, and Tinawi [2003]. The latest [2013] version of CADAM, implementing the standard vibration properties presented in Appendix A, is available for download from:

http://www.polymtl.ca/structures/telecharg/cadam/telechargement.php

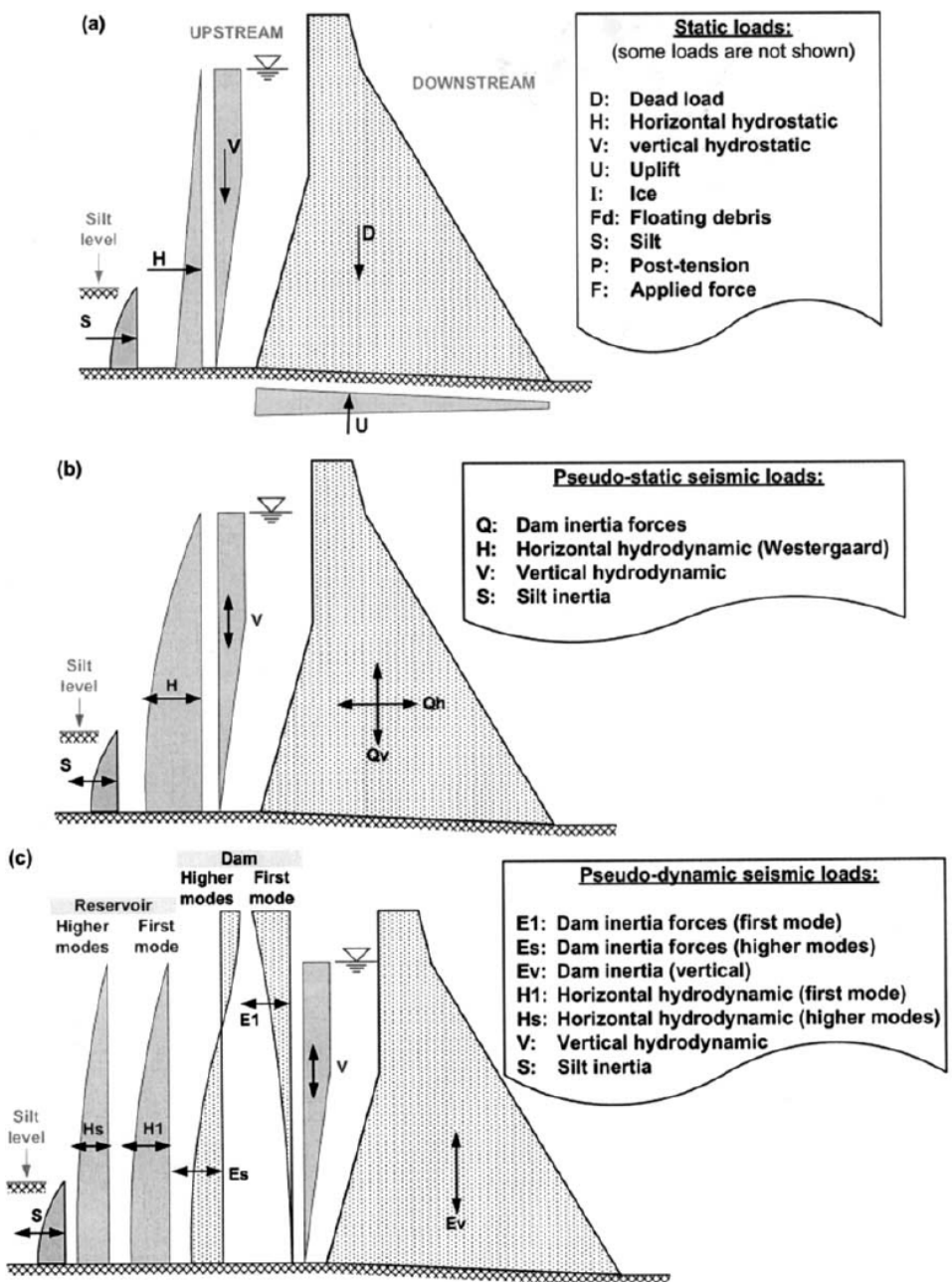

Figure 5.2 **CADAM loading conditions for static and seismic analyses: (a) basic static analysis conditions; (b) pseudo-static seismic analysis; (c) pseudo-dynamic (or RSA) seismic analysis. From Leclerc, Legér, and Tinawi [2003].**

6 Evaluation of Response Spectrum Analysis Procedure

Although based on structural dynamics theory, the RSA procedure involves several approximations which have been checked individually [Fenves and Chopra 1985a, 1985b]. Presented in this chapter is an overall evaluation of the procedure, by comparing its results with those obtained from response history analysis (RHA) of the dam modeled as a finite element system, including dam-water-foundation interaction and reservoir bottom absorption [Fenves and Chopra 1984b]; the later set of results were computed by a newer version of the program EAGD-84 [Fenves and Chopra 1984c].

6.1 SYSTEM CONSIDERED

The system considered is the tallest, non-overflow monolith of Pine Flat Dam shown in Figure 6.1, with the following properties: height of the dam, H_s = 400 ft; modulus of elasticity of concrete, E_s = 3.25 million psi; unit weight of concrete, w_s = 155 pcf; viscous damping ratio for the dam alone, ζ_1 = 2%; modulus of elasticity of the foundation, E_f = 3.25 million psi; constant hysteretic damping factor for the foundation, η_f = 0.04 (corresponding to 2% viscous damping); depth of water, H = 381 ft; and wave reflection coefficient at the reservoir bottom, α = 0.75.

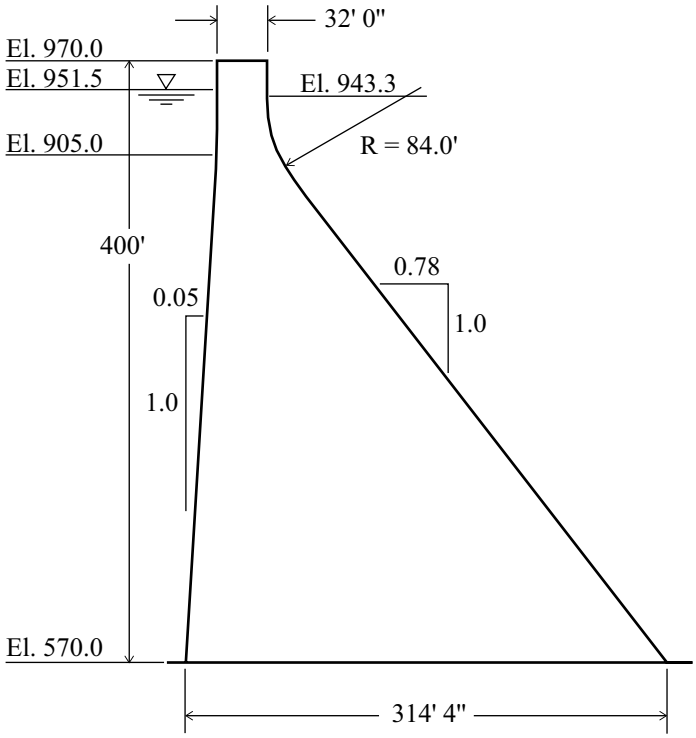

Figure 6.1 Tallest, non-overflow monolith of Pine Flat Dam.

6.2 GROUND MOTIONS

Based on a probabilistic seismic hazard analysis (PSHA) for the Pine Flat Dam site at the 1% in 100 years hazard level, a Conditional Mean Spectrum was developed. A total of 29 ground motion records on rock or NEHERP soil class D or stiffer sites, at a distance R = 0–50 km from earthquakes of magnitude M_w = 5.0–7.5 were selected; the selected range of M_w and R is consistent with the deaggregation of the seismic hazard at the site. Each of the resulting 58 ground motions (two horizontal components of 29 records) was amplitude-scaled to minimize the mean square difference between the response spectrum and the target spectrum over the period range of interest $0.3 \leq T \leq 0.5$ sec. A summary of the PSHA, as well as the selection and scaling of records is presented in Appendix B. The median (computed as the geometric mean) of the response spectra for the 58 ground motions is presented in Figure 6.2.

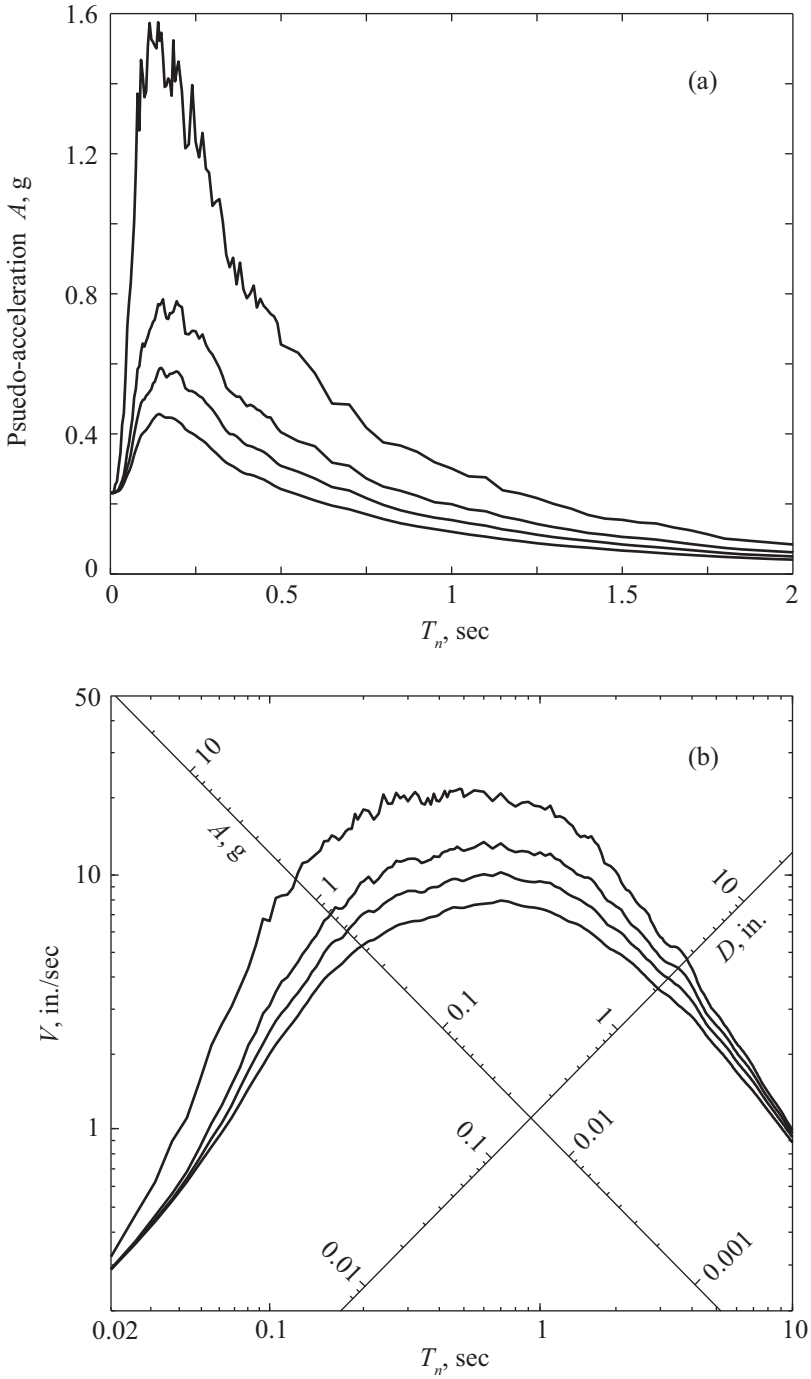

Figure 6.2 **Median response spectra for 58 ground motions: ζ = 0, 2, 5, and 10 percent; (a) linear plot; (b) four-way logarithmic plot.**

6.3 RESPONSE SPECTRUM ANALYSIS

6.3.1 Equivalent Static Lateral Forces

With the earthquake excitation defined by the median response spectrum of Figure 6.2, the dam is analyzed by the RSA procedure for the four cases listed in Table 6.1; for this purpose the step-by-step procedure described in Chapter 4 is implemented (see Appendix C for details). The vibration period and damping ratio of the equivalent SDF system with the corresponding spectral ordinates are presented in Table 6.1, and the equivalent static lateral forces $f_1(y)$ and $f_{sc}(y)$, representing the maximum earthquake effects of the fundamental and higher modes of vibration, respectively, are presented in Figure 6.3.

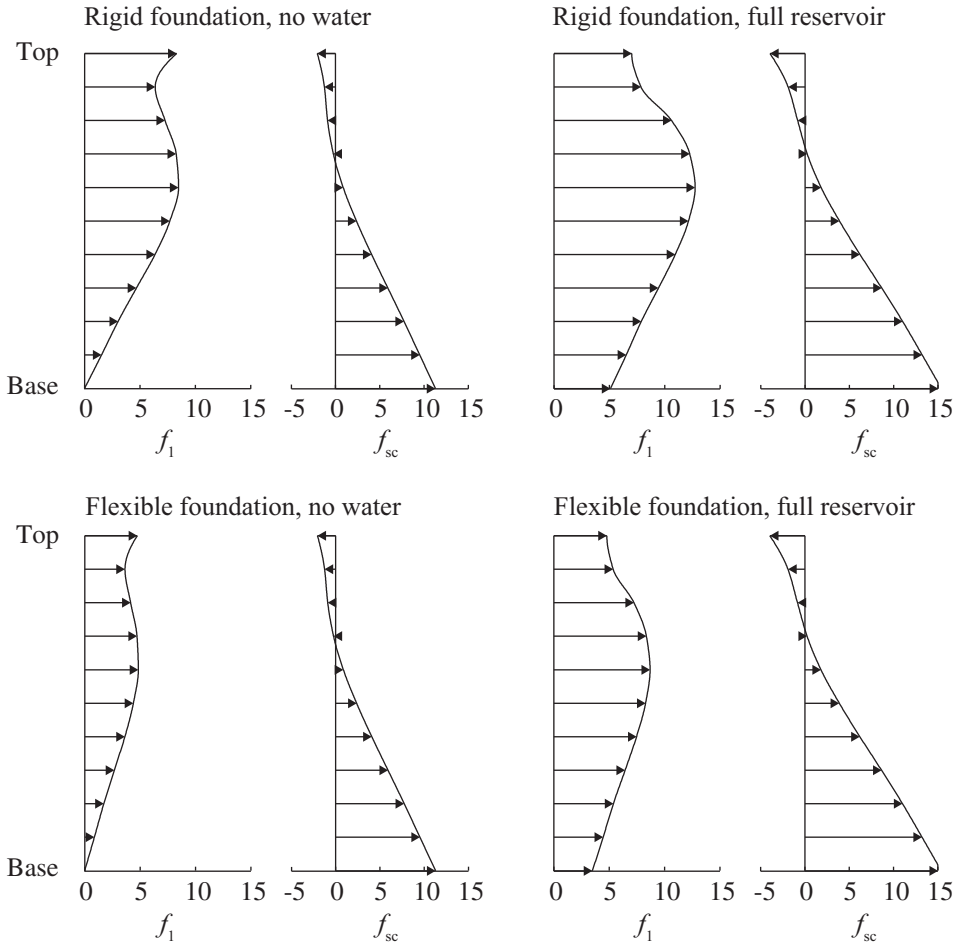

Figure 6.3 **Equivalent static lateral forces, f_1 and f_{sc}, on Pine Flat Dam, in kips per foot height, computed by the RSA procedure for four analysis cases.**

Table 6.1 **Pine Flat Dam analysis cases, fundamental mode properties, and corresponding pseudo-acceleration ordinates.**

Analysis Case	Foundation	Water	$\tilde{T}_1$, in sec	$\tilde{\zeta}_1$, in percent	$A(\tilde{T}_1, \tilde{\zeta}_1)$, in g
1	Rigid	Empty	0.311	2.0	0.606
2	Rigid	Full	0.387	3.9	0.409
3	Flexible	Empty	0.369	7.1	0.347
4	Flexible	Full	0.459	9.2	0.274

6.3.2 Computation of Stresses

The vertical stresses $\sigma_{y,1}$ and $\sigma_{y,sc}$ due to the two sets of forces f_1 and f_{sc} are computed by static stress analysis of the dam by two methods: (1) elementary formulas for stresses in beams; and (2) finite element analysis of the dam. Combining $\sigma_{y,1}$ and $\sigma_{y,sc}$ by the SRSS combination rule leads to the earthquake induced vertical stresses, $\sigma_{y,d}$, presented in Figure 6.4; note that stresses due to initial static loads are not included. The stress values presented occur as tensile stresses at the upstream face when the earthquake forces act in the downstream direction, and at the downstream face when the earthquake forces act in the upstream direction. A detailed description of the computational procedure is included in Appendix C.

The results presented in Figure 6.4 confirm that the correction factor of 0.75 for stresses computed by beam theory at the sloping part of the downstream face is satisfactory for all four cases. The stresses determined by beam theory with the correction factor are very close to those determined by finite element analysis except near the heel and toe of the dam. Therefore, only the stresses from RSA determined by beam theory are compared with the results from RHA in Section 6.4.2.

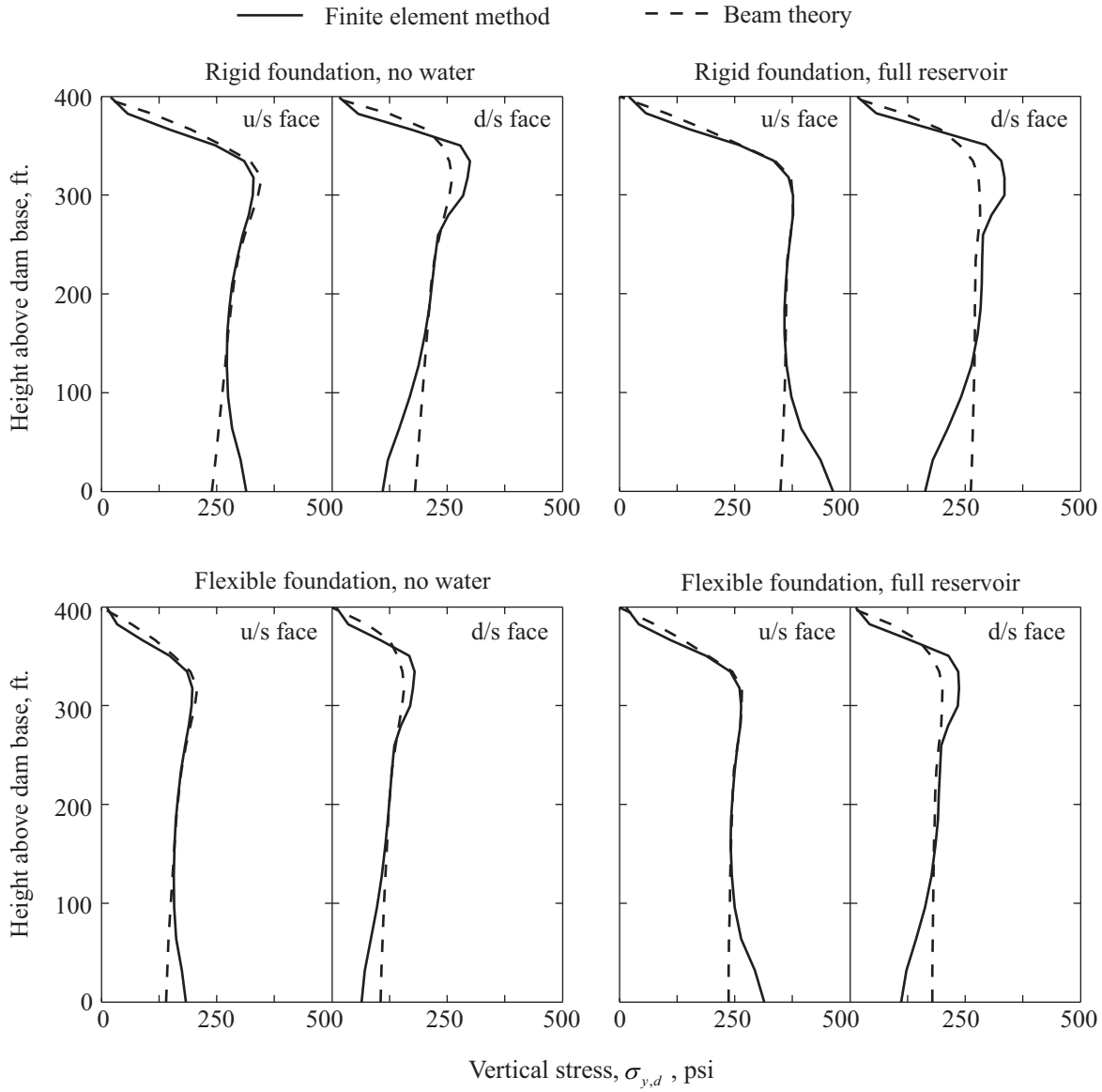

Figure 6.4 **Earthquake induced vertical stresses, $\sigma_{y,d}$, in Pine Flat Dam computed in the RSA procedure by two methods: beam theory and the finite element method.**

6.4 COMPARISON WITH RESPONSE HISTORY ANALYSIS

Response history analysis of the dam monolith modeled as a finite element system, considering rigorously the effects of dam-water-foundation interaction and reservoir bottom absorption, is implemented by a newer version of the computer program EAGD-84 [Fenves and Chopra 1984c] for each of the 58 ground motions. In the following sections, results computed by RSA and RHA procedures are compared.

6.4.1 Fundamental Mode Properties

The fundamental vibration period and the effective damping ratio at this period are estimated using Equations (2.6) - (2.9) in the RSA procedure. These vibration properties are not needed in the RHA procedure; however, for the purposes of evaluating the accuracy of the approximate results, they are determined—by the half-power bandwidth method—from the frequency response function for the fundamental mode response of the dam-water-foundation system computed in the EAGD-84 program. These are referred to as the "exact" results in Table 6.2.

It is apparent that the approximate procedure provides excellent estimates for the resonant period and effective damping ratio of the system in its fundamental mode, confirming that the equivalent SDF model for the dam-water-foundation system is able to represent the important effects of dam-water interaction, reservoir bottom absorption and dam-foundation interaction.

Table 6.2 "Exact" and approximate fundamental mode properties.

			Vibration Period, $\tilde{T}_1$, in sec		Damping Ratio, $\tilde{\zeta}_1$, in percent	
Case	Foundation	Water	Approx.	Exact	Approx.	Exact
1	Rigid	Empty	0.311	0.318	2.0	2.0
2	Rigid	Full	0.387	0.395	3.9	3.2
3	Flexible	Empty	0.369	0.390	7.1	8.7
4	Flexible	Full	0.459	0.491	9.2	9.8

6.4.2 Stresses

The peak value of the maximum principal stress at a location over the duration of each ground motion is determined from the response history computed by the EAGD-84 program, see Appendix C. At the two faces of the dam, the principal stresses are essentially parallel to the faces if the upstream face is nearly vertical and the stresses due to tail-water at the downstream face are negligible [Fenves and Chopra 1986]; these conditions are usually satisfied in practical problems. This implies that the direction of the peak value of maximum principal stress at locations on a dam face is essentially invariant among ground motions, therefore the peak stress values due to the 58 ground motions lend themselves to statistical analysis.

At each location on the two faces of the dam the median value is computed as the geometric mean of the data set; results are presented in Figure 6.5 where they are compared with the RSA results. The maximum principal stresses in the RSA procedure are obtained by a transformation of the vertical stresses determined by beam theory.

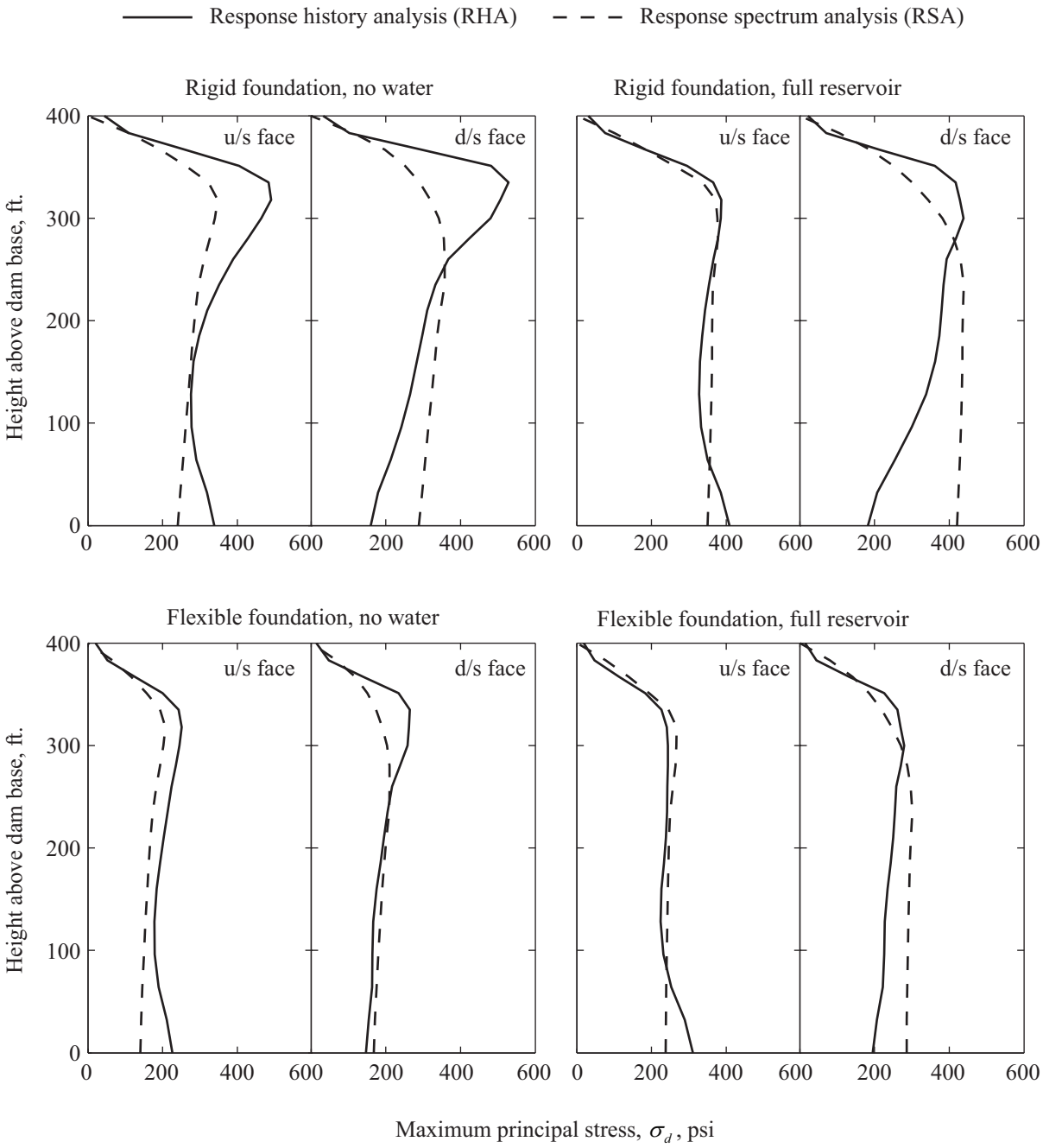

Figure 6.5 **Comparison of peak values of maximum principal stresses in Pine Flat Dam computed by RSA and RHA procedures; initial static stresses are excluded.**

Case 1 (rigid foundation, empty reservoir) is an example where higher mode contributions are considerable, primarily in the upper part of the dam, as expected, where the steep stress gradients are evident in the RHA results (Figure 6.5). The RSA procedure

underestimates these higher mode contributions because the vibration periods are not short enough for the static correction approximation to be valid. As shown in Figure 6.6, the spectral accelerations at the second- and third-mode periods are more than three times the peak ground acceleration that is used instead in the static correction method. Thus, the static correction method grossly underestimates the higher mode stresses. For the median response spectrum considered, such discrepancy would be much smaller in the case of a dam of lower height with shorter periods. For Cases 2–4 the RSA procedure provides very good estimates of the maximum principal stresses.

The RSA procedure tends to be more conservative—relative to the RHA results—at the downstream face of the dam than at the upstream face (Figure 6.5). An investigation revealed that the underlying reason is the one-dimensional representation of the equivalent static lateral forces in Equation (2.1), wherein any variation of the fundamental mode shape over the breadth of the dam was neglected, thus ignoring the horizontal variation of the lateral forces.

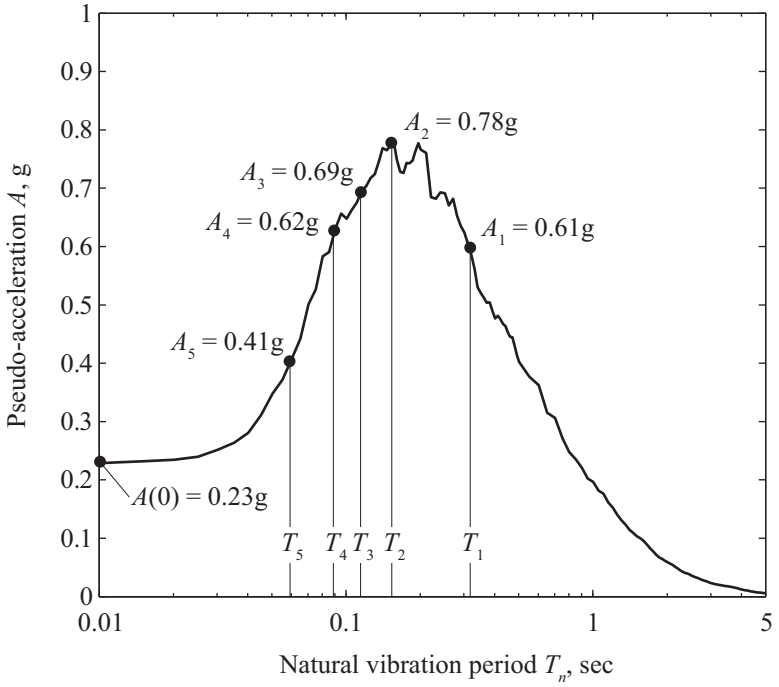

Figure 6.6 Spectral accelerations at the first five natural vibration periods of Pine Flat Dam on rigid foundation with empty reservoir; damping, ζ = 2%.

The preceding results demonstrate that the RSA procedure estimates stresses to a degree of accuracy that is satisfactory for the preliminary phase in the design of new dams and in the safety evaluation of existing dams. The level of accuracy achieved in the RSA procedure is noteworthy, especially considering the complicated effects of dam-water-foundation interaction and reservoir bottom absorption on the dynamics of the system, and the number of approximations necessary to develop the procedure. The accuracy of the computed results

depends on several factors, including how well the fundamental resonant period and damping ratio are estimated in the RSA procedure, and how well the static correction method is able to account for the contributions from higher modes to the total response.

7 Conclusions

Two analysis procedures are available for earthquake analysis of concrete gravity dams including dam-water-foundation interaction: (1) response spectrum analysis (RSA) in which the peak response is estimated directly from the earthquake design spectrum; and (2) response history analysis (RHA) of a finite element idealization of the dam monolith. The investigation presented in this report has led to the following conclusions:

1. Analyses of an actual dam to an ensemble of 58 ground motions has demonstrated that the RSA procedure estimates dam response that is close enough to the "exact" response determined by the RHA procedure. Thus, the RSA procedure is satisfactory for the preliminary phase of the design of new dams and in the safety evaluation of existing dams.
2. To enhance the accuracy of this RSA procedure, the possibility of calculating stresses by finite element analysis versus the commonly used beam formulas was investigated, and a correction factor for beam stresses on the downstream face of the dam has been developed.
3. A more complete set of data for the parameters that characterize dam-foundation interaction in the RSA procedure has been developed. Availability of these data should provide sufficient control over the overall damping in the dam-water-foundation system to ensure consistency with damping measured from motions of dams recorded during forced vibration tests and earthquakes.

REFERENCES

Alves S.W., Hall J.F. (2006). System identification of a concrete arch dam and the calibration of its finite element model, *Earthq. Eng. Struct. Dyn.,* 35(11): 1321–1337.

Baker J. (2011). Conditional Mean Spectrum: Tool for ground motion selection, *J. Struct. Eng.*, ASCE, 137: 322–331

Baker J., Cornell C.A. (2006). Spectral shape, epsilon and record selection, *Earthq. Eng. Struct. Dyn.*, 35: 1077–1095.

Chakrabarti P., Chopra A.K. (1973). Earthquake analysis of gravity dams including hydrodynamic interaction, *Earthq. Eng. Struct. Dyn.*, 2: 143–160.

Chopra A.K. (2012). *Dynamics of Structures: Theory and Applications to Earthquake Engineering*, 4th ed., Prentice Hall, Upper Saddle River, NJ.

Chopra A.K. (1978). Earthquake resistant design of concrete gravity dams, *J. Struct. Div.*, ASCE, 104(ST6): 953–971.

Chopra A.K., Wang J-T. (2010). Linear analysis of concrete arch dams including dam–water–foundation rock interaction considering spatially varying ground motions, *Earthq. Eng. Struct. Dyn.,* 39(7):731-75.

Fenves G., Chopra A.K. (1987). Simplified earthquake analysis of concrete gravity dams, *J. Struct. Eng.*, ASCE, 113(8):,1688-1708.

Fenves G., Chopra A.K. (1986). Simplified analysis for earthquake-resistant design of concrete gravity dams, *Report No. UCB/EERC-85/10*, Earthquake Engineering Research Center, University of California, Berkeley, Calif., 149 pgs.

Fenves G., Chopra A.K. (1985a). Simplified earthquake analysis of concrete gravity dams: Separate hydrodynamic and foundation interaction effects, *J. Eng. Mech.*, ASCE, 111(6): 715–735.

Fenves G., Chopra A.K. (1985b). Simplified earthquake analysis of concrete gravity dams: Combined hydrodynamic and foundation interaction effects, *J. Eng. Mech.*, ASCE, 111(6): 736–756.

Fenves G., Chopra A.K. (1984a). Earthquake analysis and response of concrete gravity dams, *Report No. UCB/EERC-84/10,* Earthquake Engineering Research Center, University of California, Berkeley, CA, 213 pgs.

Fenves G., Chopra A.K. (1984b). Earthquake analysis of concrete gravity dams including reservoir bottom absorption and dam-water-foundation rock interaction, *Earthq. Eng. Struct. Dyn.*, 12(5):663–680.

Fenves G., Chopra A.K. (1984c). EAGD-84: A computer program for earthquake response analysis of concrete gravity dams, *Report No. UCB/EERC-84/11,* Earthquake Engineering Research Center, University of California, Berkeley, CA, 78 pgs.

Fenves G., Chopra A.K. (1983). Effects of reservoir bottom absorption on earthquake response of concrete gravity dams, *Earthq. Eng. Struct. Dyn.*, 11(6): 809–829.

Leclerc M., Léger P., Tinawi R. (2003). Computer aided stability analysis of gravity dams – CADAM, *Adv. Eng. Software*, 34(7): 403–420.

Leclerc M., Léger P., Tinawi R. (2002). Computer aided stability analysis of gravity dams, *Proceedings, 4th Structural Specialty Conference of the Canadian Society for Civil Engineering,* Montréal, Québec, Canada.

Proulx J, et. al. (2001). An experimental investigation of water level effects on the dynamic behavior of a large arch dam, *Earthq. Eng. Struct. Dyn.*, 30(8): 1147–1166.

PEER Ground Motion (2010): PEER Ground Motion Database, Pacific Earthquake Engineering Research Center, http://peer.berkeley.edu/peer_ground_motion_database/

Rea, D., Liaw C-Y., Chopra A.K. (1975). Mathematical models for the dynamic analysis of concrete gravity dams, *Earthq. Eng. Struct. Dyn.*, 3(3): 249–258.

USGS Deaggregation (2008). PSHA Interactive Deaggregation Tool, U.S. Geological Survey, https://geohazards.usgs.gov/deaggint/2008/documentation.php.

Veletsos A.S. (1977). Dynamics of structure-foundation systems, in: *Structural and Geotechnical Mechanics*, ed., W.J. Hall, Prentice-Hall, Clifton, New Jersey.

NOTATION

The following symbols are used in this report:

$A\left(\tilde{T}_1, \tilde{\zeta}_1\right)$	pseudo-acceleration spectrum ordinate evaluated at natural period $\tilde{T}_1$ and damping ratio $\tilde{\zeta}_1$
A_p	integral of $2gp(\hat{y})/wH$ over depth of the impounded water for $H/H_s = 1$ as listed in Table A.5
a_g	peak ground acceleration
B_1	defined in Equation (2.11)
C	velocity of pressure waves in water
E_f	Young's modulus of elasticity of foundation rock
E_s	Young's modulus of elasticity of dam concrete
F_{st}	$= ½wH^2$, hydrostatic force
$f_1(y)$	equivalent static lateral forces acting on the upstream face of the dam due to the fundamental mode of vibration, as defined in Equation (2.1)
$f_{sc}(y)$	equivalent static lateral forces acting on the upstream face of the dam due to higher modes of vibration, as defined in Equation (2.10)
g	acceleration due to gravity
H	depth of impounded water
H_s	height of upstream face of dam
L_1	generalized earthquake force coefficient, defined in Equation (2.5)
$\tilde{L}_1$	integral defined in Equation (2.3)
M_1	generalized mass of dam, defined in Equation (2.4)
$\tilde{M}_1$	integral defined in Equation (2.2)
$p\left(y, \tilde{T}_r\right)$	real-valued component of the complex-valued function representing the hydrodynamic pressure on the upstream face due to harmonic acceleration at period $\tilde{T}_r$ in the shape of the fundamental mode
$p_0(y)$	hydrodynamic pressure on a rigid dam with water compressibility neglected
R_f	period lengthening ratio due to dam-foundation interaction
R_r	period lengthening ratio due to dam-water interaction
R_w	$= T_1^r / \tilde{T}_r$
r_1	response due to earthquake forces associated with the fundamental mode of vibration
r_{max}	peak earthquake response of the dam including initial static effects
r_{sc}	response due to earthquake forces associated with the higher modes of vibration
r_{st}	response due to initial static effects
T_1	fundamental vibration period of dam on rigid foundation with empty reservoir given by Equation (3.1)
$\tilde{T}_1$	fundamental resonant period of dam on flexible foundation with impounded water given by Equation (2.8)
T_1^r	$= 4H/C$, fundamental vibration period of impounded water

$\tilde{T}_f$	fundamental resonant period of dam on flexible foundation with empty reservoir given by Equation (2.7)
$\tilde{T}_r$	fundamental resonant period of dam on rigid foundation with impounded water given by Equation (2.6)
t	time
w	unit weight of water
$w_s(y)$	weight of dam per unit height
x	coordinate along the breadth of the dam
y	coordinate along the height of the dam
$\hat{y}$	$= y / H$
α	wave reflection coefficient for reservoir bottom materials
$\tilde{\Gamma}_1$	$= \tilde{L}_1 / \tilde{M}_1$
$\phi_1(y)$	fundamental vibration mode shape of dam at upstream face
η_f	constant hysteretic damping factor for foundation rock
ζ_1	damping ratio of dam on rigid foundation with empty reservoir
$\tilde{\zeta}_1$	damping ratio for dam on flexible foundation with impounded water
$\tilde{\zeta}_f$	added damping due to dam-foundation interaction
$\tilde{\zeta}_r$	added damping due to dam-water interaction
$\sigma_{y,1}$	vertical stress due to earthquake forces associated with the fundamental mode of vibration
$\sigma_{y,d}$	earthquake induced vertical stress
$\sigma_{y,sc}$	vertical stress due to earthquake forces associated with the higher modes of vibration
σ_d	peak value of maximum principal stress

Appendix A Tables for Standard Values Used in Analysis Procedure

Table A.1 Standard fundamental mode shape $\phi_1(y)$ for concrete gravity dams.

y/H_s	$\phi_1(y)$
1.0	1.000
0.95	.866
0.90	.735
0.85	.619
0.80	.530
0.75	.455
0.70	.389
0.65	.334
0.60	.284
0.55	.240
0.50	.200
0.45	.165
0.40	.135
0.35	.108
0.30	.084
0.25	.065
0.20	.047
0.15	.034
0.10	.021
0.05	.010
0	0

Table A.2(a) Standard values for R_r and ζ_r, the period lengthening ratio and added damping ratio due to hydrodynamic effects for modulus of elasticity of concrete, E_s = 5 and 4.5 million psi.

		E_s = 5 million psi		E_s = 4.5 million psi	
H/H_s	α	R_r	ζ_r	R_r	ζ_r
1.0	1.0	1.454	0	1.409	0
	0.90	1.462	.043	1.416	.030
	0.75	1.456	.060	1.412	.051
	0.50	1.355	.067	1.344	.060
	0.25	1.284	.054	1.285	.050
	0	1.261	.038	1.259	.036
0.95	1.0	1.368	0	1.323	0
	0.90	1.376	.044	1.330	.031
	0.75	1.366	.056	1.323	.049
	0.50	1.255	.060	1.256	.053
	0.25	1.208	.045	1.208	.042
	0	1.192	.032	1.191	.030
0.90	1.0	1.289	0	1.247	0
	0.90	1.297	.041	1.253	.029
	0.75	1.284	.050	1.247	.042
	0.50	1.181	.050	1.185	.044
	0.25	1.151	.036	1.152	.033
	0	1.139	.025	1.139	.023
0.85	1.0	1.215	0	1.179	0
	0.90	1.224	.033	1.185	.023
	0.75	1.206	.042	1.177	.034
	0.50	1.129	.039	1.131	.033
	0.25	1.111	.027	1.109	.025
	0	1.100	.019	1.099	.018
0.80	1.0	1.148	0	1.121	0
	0.90	1.156	.024	1.126	.015
	0.75	1.140	.032	1.121	.024
	0.50	1.092	.028	1.092	.024
	0.25	1.078	.019	1.078	.018
	0	1.071	.014	1.071	.013
0.75	1.0	1.092	0	1.078	0
	0.90	1.099	.014	1.080	.008
	0.75	1.089	.021	1.078	.014
	0.50	1.065	.018	1.064	.015
	0.25	1.055	.013	1.055	.012
	0	1.049	.009	1.050	.009

Table A.2(a) – continued.

		E_s = 5 million psi		E_s = 4.5 million psi	
H/H_s	α	R_r	ζ_r	R_r	ζ_r
0.70	1.0	1.055	0	1.048	0
	0.90	1.057	.006	1.050	.003
	0.75	1.055	.011	1.050	.007
	0.50	1.045	.011	1.044	.009
	0.25	1.038	.009	1.037	.008
	0	1.034	.006	1.035	.006
0.65	1.0	1.033	0	1.031	0
	0.90	1.034	.002	1.031	.001
	0.75	1.034	.005	1.031	.003
	0.50	1.030	.006	1.029	.005
	0.25	1.026	.005	1.027	.005
	0	1.024	.004	1.025	.004
0.60	1.0	1.020	0	1.020	0
	0.90	1.020	.001	1.020	.001
	0.75	1.020	.002	1.020	.001
	0.50	1.019	.003	1.018	.003
	0.25	1.017	.003	1.018	.003
	0	1.016	.003	1.016	.002
0.55	1.0	1.013	0	1.012	0
	0.90	1.013	.000	1.012	.000
	0.75	1.013	.001	1.012	.001
	0.50	1.013	.002	1.012	.001
	0.25	1.012	.002	1.012	.002
	0	1.011	.002	1.012	.001
0.50	1.0	1.009	0	1.008	0
	0.90	1.009	.000	1.008	.000
	0.75	1.009	.000	1.008	.000
	0.50	1.008	.001	1.008	.001
	0.25	1.008	.001	1.008	.001
	0	1.008	.001	1.008	.001

Table A.2(b) Standard values for R_r and ζ_r, the period lengthening ratio and added damping ratio due to hydrodynamic effects for modulus of elasticity of concrete, E_s = 4, 3.5 and 3 million psi.

		E_s = 4 million psi		E_s = 3.5 million psi		E_s = 3 million psi	
H/H_s	α	R_r	ζ_r	R_r	ζ_r	R_r	ζ_r
1.0	1.0	1.370	0	1.341	0	1.320	0
	0.90	1.374	.021	1.344	.013	1.319	.008
	0.75	1.374	.040	1.341	.029	1.312	.021
	0.50	1.333	.051	1.316	.042	1.289	.035
	0.25	1.285	.045	1.282	.040	1.264	.036
	0	1.259	.034	1.256	.032	1.247	.030
0.95	1.0	1.289	0	1.259	0	1.241	0
	0.90	1.292	.020	1.263	.012	1.240	.007
	0.75	1.289	.038	1.259	.027	1.233	.019
	0.50	1.247	.045	1.238	.036	1.213	.030
	0.25	1.208	.038	1.208	.033	1.194	.030
	0	1.191	.028	1.188	.026	1.181	.025
0.90	1.0	1.214	0	1.191	0	1.176	0
	0.90	1.220	.017	1.193	.010	1.176	.006
	0.75	1.214	.033	1.193	.022	1.171	.015
	0.50	1.179	.037	1.174	.029	1.155	.024
	0.25	1.152	.030	1.152	.026	1.141	.024
	0	1.139	.022	1.136	.020	1.131	.019
0.85	1.0	1.152	0	1.136	0	1.126	0
	0.90	1.157	.013	1.139	.007	1.125	.004
	0.75	1.155	.024	1.136	.016	1.122	.011
	0.50	1.129	.028	1.124	.023	1.111	.017
	0.25	1.109	.022	1.109	.020	1.101	.017
	0	1.099	.017	1.099	.016	1.093	.015
0.80	1.0	1.104	0	1.095	0	1.087	0
	0.90	1.106	.008	1.094	.004	1.087	.003
	0.75	1.106	.016	1.090	.011	1.085	.007
	0.50	1.089	.019	1.080	.016	1.079	.012
	0.25	1.078	.016	1.071	.014	1.071	.012
	0	1.071	.012	1.066	.011	1.066	.011
0.75	1.0	1.070	0	1.063	0	1.059	0
	0.90	1.069	.004	1.063	.003	1.059	.002
	0.75	1.065	.010	1.061	.006	1.058	.004
	0.50	1.056	.013	1.055	.010	1.054	.007
	0.25	1.050	.011	1.050	.010	1.050	.008
	0	1.046	.009	1.046	.008	1.046	.007

Table A.2(b) – continued.

		E_s = 4 million psi		E_s = 3.5 million psi		E_s = 3 million psi	
H/H_s	α	R_r	ζ_r	R_r	ζ_r	R_r	ζ_r
0.70	1.0	1.044	0	1.041	0	1.039	0
	0.90	1.044	.002	1.041	.001	1.039	.001
	0.75	1.042	.005	1.040	.003	1.038	.002
	0.50	1.038	.007	1.037	.006	1.036	.004
	0.25	1.034	.007	1.034	.006	1.034	.005
	0	1.031	.006	1.031	.005	1.031	.005
0.65	1.0	1.028	0	1.026	0	1.025	0
	0.90	1.028	.001	1.026	.001	1.025	.000
	0.75	1.027	.002	1.026	.002	1.025	.001
	0.50	1.025	.004	1.024	.003	1.024	.002
	0.25	1.023	.004	1.022	.004	1.022	.003
	0	1.021	.004	1.021	.003	1.021	.003
0.60	1.0	1.017	0	1.016	0	1.016	0
	0.90	1.017	.000	1.016	.000	1.016	.000
	0.75	1.017	.001	1.016	.001	1.016	.001
	0.50	1.016	.002	1.015	.002	1.015	.001
	0.25	1.015	.002	1.014	.002	1.014	.002
	0	1.013	.002	1.013	.002	1.013	.002
0.55	1.0	1.010	0	1.010	0	1.010	0
	0.90	1.010	.000	1.010	.000	1.010	.000
	0.75	1.010	.001	1.010	.000	1.010	.000
	0.50	1.010	.001	1.010	.001	1.009	.001
	0.25	1.009	.001	1.009	.001	1.009	.001
	0	1.009	.001	1.009	.001	1.009	.001
0.50	1.0	1.006	0	1.006	0	1.006	0
	0.90	1.006	.000	1.006	.000	1.006	.000
	0.75	1.006	.000	1.006	.000	1.006	.000
	0.50	1.006	.001	1.006	.001	1.006	.001
	0.25	1.005	.001	1.005	.001	1.005	.001
	0	1.005	.001	1.005	.001	1.005	.001

Table A.2(c) Standard values for R_r and ζ_r, the period lengthening ratio and added damping ratio due to hydrodynamic effects for modulus of elasticity of concrete, E_s = 2.5, 2 and 1 million psi.

		E_s = 2.5 million psi		E_s = 2 million psi		E_s = 1 million psi	
H/H_s	α	R_r	ζ_r	R_r	ζ_r	R_r	ζ_r
1.0	1.0	1.301	0	1.286	0	1.263	0
	0.90	1.301	.005	1.285	.003	1.263	.001
	0.75	1.287	.014	1.284	.009	1.262	.004
	0.50	1.283	.025	1.275	.018	1.260	.008
	0.25	1.264	.030	1.262	.024	1.256	.013
	0	1.247	.027	1.247	.024	1.247	.017
0.95	1.0	1.224	0	1.212	0	1.193	0
	0.90	1.224	.005	1.211	.003	1.193	.001
	0.75	1.221	.012	1.210	.008	1.193	.003
	0.50	1.209	.022	1.203	.015	1.191	.007
	0.25	1.194	.025	1.192	.020	1.187	.011
	0	1.181	.022	1.181	.020	1.181	.014
0.90	1.0	1.164	0	1.154	0	1.140	0
	0.90	1.163	.004	1.154	.002	1.140	.001
	0.75	1.161	.009	1.152	.006	1.140	.002
	0.50	1.152	.017	1.148	.012	1.139	.005
	0.25	1.141	.020	1.140	.016	1.136	.008
	0	1.131	.018	1.131	.016	1.131	.011
0.85	1.0	1.117	0	1.110	0	1.100	0
	0.90	1.116	.003	1.110	.002	1.100	.001
	0.75	1.115	.007	1.109	.004	1.100	.002
	0.50	1.109	.012	1.106	.009	1.100	.004
	0.25	1.101	.014	1.100	.012	1.097	.006
	0	1.093	.013	1.093	.012	1.093	.008
0.80	1.0	1.081	0	1.077	0	1.071	0
	0.90	1.081	.002	1.077	.001	1.071	.000
	0.75	1.080	.004	1.076	.003	1.071	.001
	0.50	1.076	.008	1.074	.006	1.070	.003
	0.25	1.071	.010	1.071	.008	1.069	.005
	0	1.066	.010	1.066	.008	1.066	.006
0.75	1.0	1.055	0	1.053	0	1.049	0
	0.90	1.055	.001	1.053	.001	1.049	.000
	0.75	1.054	.003	1.052	.002	1.049	.001
	0.50	1.053	.005	1.051	.004	1.048	.002
	0.25	1.050	.007	1.049	.005	1.048	.003
	0	1.046	.007	1.046	.006	1.046	.004

Table A.2(c) – continued.

		E_s = 2.5 million psi		E_s = 2 million psi		E_s = 1 million psi	
H/H_s	α	R_r	ζ_r	R_r	ζ_r	R_r	ζ_r
0.70	1.0	1.037	0	1.035	0	1.033	0
	0.90	1.037	.001	1.035	.000	1.033	.000
	0.75	1.037	.002	1.035	.001	1.033	.000
	0.50	1.035	.003	1.034	.002	1.033	.001
	0.25	1.033	.004	1.033	.004	1.032	.002
	0	1.031	.004	1.031	.004	1.031	.003
0.65	1.0	1.024	0	1.023	0	1.022	0
	0.90	1.024	.000	1.023	.000	1.022	.000
	0.75	1.024	.001	1.023	.001	1.022	.000
	0.50	1.023	.002	1.023	.001	1.022	.001
	0.25	1.022	.003	1.022	.002	1.021	.001
	0	1.021	.003	1.021	.003	1.021	.002
0.60	1.0	1.016	0	1.016	0	1.014	0
	0.90	1.016	.000	1.016	.000	1.014	.000
	0.75	1.016	.001	1.016	.001	1.014	.000
	0.50	1.015	.001	1.015	.001	1.014	.000
	0.25	1.014	.002	1.014	.002	1.014	.001
	0	1.013	.002	1.013	.002	1.013	.001
0.55	1.0	1.009	0	1.009	0	1.009	0
	0.90	1.009	.000	1.009	.000	1.009	.000
	0.75	1.009	.000	1.009	.000	1.009	.000
	0.50	1.009	.001	1.009	.000	1.009	.000
	0.25	1.009	.001	1.009	.001	1.009	.000
	0	1.009	.001	1.009	.001	1.009	.001
0.50	1.0	1.006	0	1.006	0	1.005	0
	0.90	1.006	.000	1.006	.000	1.005	.000
	0.75	1.006	.000	1.006	.000	1.005	.000
	0.50	1.006	.000	1.005	.000	1.005	.000
	0.25	1.005	.000	1.005	.000	1.005	.000
	0	1.005	.001	1.005	.000	1.005	.000

Table A.3 **Standard values for R_f and ζ_f, the period lengthening ratio and added damping ratio due to dam-foundation interaction.**

		Added damping ratio, ζ_f									
E_f / E_s	R_f	η_f =.01	η_f =.02	η_f =.03	η_f =.04	η_f =.05	η_f =.06	η_f =.07	η_f =.08	η_f =.09	η_f =.10
5.0	1.044	.011	.011	.011	.012	.012	.013	.013	.013	.014	.014
4.5	1.049	.012	.012	.013	.013	.014	.014	.015	.015	.015	.016
4.0	1.054	.013	.014	.014	.015	.015	.016	.016	.017	.017	.018
3.5	1.061	.016	.016	.017	.017	.018	.018	.019	.019	.020	.020
3.0	1.070	.018	.019	.020	.020	.021	.021	.022	.023	.023	.024
2.5	1.083	.022	.023	.024	.024	.025	.026	.026	.027	.028	.028
2.0	1.102	.028	.029	.030	.030	.031	.032	.033	.034	.035	.035
1.5	1.131	.037	.038	.039	.040	.041	.042	.043	.045	.046	.047
1.4	1.139	.040	.041	.042	.043	.044	.045	.046	.048	.049	.050
1.3	1.149	.043	.044	.045	.046	.047	.049	.050	.051	.052	.053
1.2	1.159	.046	.047	.049	.050	.051	.052	.054	.055	.056	.057
1.1	1.172	.050	.051	.053	.054	.055	.057	.058	.059	.061	.062
1.0	1.187	.054	.056	.057	.059	.060	.062	.063	.065	.066	.067
0.9	1.204	.060	.062	.063	.065	.066	.068	.069	.071	.072	.074
0.8	1.225	.066	.068	.070	.072	.073	.075	.077	.078	.080	.082
0.7	1.252	.075	.076	.078	.080	.082	.084	.086	.087	.089	.091
0.6	1.286	.085	.087	.089	.091	.093	.095	.097	.099	.101	.103
0.5	1.332	.097	.100	.102	.104	.107	.109	.111	.114	.116	.118
0.4	1.396	.115	.117	.120	.123	.125	.128	.130	.133	.136	.138
0.3	1.495	.138	.141	.145	.148	.151	.154	.157	.160	.163	.166
0.2	1.670	.173	.177	.181	.185	.189	.193	.197	.201	.205	.208

Table A.3 – continued.

	Added damping ratio, ζ_f						
E_f / E_s	η_f =0.12	η_f =0.14	η_f =0.16	η_f =0.18	η_f =0.20	η_f =0.25	η_f =0.50
5.0	.015	.016	.016	.017	.018	.019	.025
4.5	.017	.017	.018	.019	.020	.021	.027
4.0	.019	.020	.020	.021	.022	.024	.030
3.5	.021	.022	.023	.024	.025	.027	.035
3.0	.025	.026	.027	.028	.029	.032	.040
2.5	.030	.031	.032	.034	.035	.038	.047
2.0	.037	.039	.040	.042	.043	.046	.058
1.5	.049	.051	.052	.054	.056	.060	.075
1.4	.052	.054	.056	.058	.060	.064	.080
1.3	.055	.058	.060	.062	.064	.068	.085
1.2	.060	.062	.064	.066	.068	.073	.091
1.1	.064	.067	.069	.072	.074	.079	.098
1.0	.070	.073	.075	.078	.080	.086	.107
0.9	.077	.080	.082	.085	.088	.094	.117
0.8	.085	.088	.091	.094	.097	.104	.129
0.7	.095	.098	.101	.105	.108	.115	.143
0.6	.107	.111	.114	.118	.121	.130	.162
0.5	.122	.127	.131	.135	.139	.149	.186
0.4	.143	.148	.153	.158	.163	.174	.220
0.3	.172	.179	.185	.191	.196	.211	.269
0.2	.216	.224	.232	.240	.247	.266	.351

Table A.4(a) Standard values for the hydrodynamic pressure function $p(\hat{y})$ for full reservoir, i.e., H/H_s = 1; α = 1.0.

	Value of $gp(\hat{y})/wH$												
$\hat{y} = y/H$	$R_w \leq .5$	$R_w = .7$	$R_w = .8$	$R_w = .85$	$R_w = .90$	$R_w = .92$	$R_w = .93$	$R_w = .94$	$R_w = .95$	$R_w = .96$	$R_w = .97$	$R_w = .98$	$R_w = .99$
1.00	0	0	0	0	0	0	0	0	0	0	0	0	0
0.95	.070	.073	.076	.079	.083	.086	.088	.090	.092	.096	.102	.111	.133
0.90	.112	.118	.124	.129	.138	.143	.147	.151	.157	.164	.176	.195	.238
0.85	.127	.135	.144	.152	.164	.172	.178	.184	.193	.204	.221	.249	.313
0.80	.133	.144	.155	.165	.182	.193	.200	.208	.220	.235	.257	.295	.379
0.75	.141	.154	.168	.180	.201	.214	.223	.234	.248	.267	.294	.340	.445
0.70	.145	.161	.178	.192	.216	.232	.242	.255	.272	.294	.327	.382	.506
0.65	.143	.161	.180	.197	.224	.242	.254	.269	.288	.313	.351	.414	.558
0.60	.139	.159	.180	.199	.230	.250	.264	.280	.301	.330	.373	.444	.605
0.55	.137	.159	.183	.203	.237	.260	.274	.293	.316	.348	.395	.473	.651
0.50	.135	.159	.184	.206	.244	.269	.284	.304	.329	.364	.415	.500	.694
0.45	.130	.155	.182	.206	.246	.272	.289	.310	.338	.375	.430	.522	.730
0.40	.124	.151	.179	.204	.247	.275	.293	.315	.345	.384	.442	.540	.762
0.35	.121	.149	.179	.205	.250	.279	.298	.322	.353	.395	.456	.559	.793
0.30	.118	.147	.178	.206	.252	.283	.303	.328	.360	.403	.467	.575	.820
0.25	.113	.143	.175	.204	.252	.284	.304	.330	.363	.408	.475	.587	.840
0.20	.109	.139	.172	.202	.252	.284	.305	.332	.366	.412	.481	.596	.856
0.15	.107	.138	.172	.202	.252	.286	.307	.334	.369	.417	.487	.604	.871
0.10	.106	.137	.172	.202	.253	.287	.309	.337	.372	.420	.491	.611	.881
0.05	.103	.135	.169	.200	.252	.286	.308	.336	.372	.420	.492	.613	.886
0	.100	.133	.168	.198	.251	.285	.307	.335	.371	.420	.492	.613	.886

Table A.4(b) Standard values for the hydrodynamic pressure function $p(\hat{y})$ for full reservoir, i.e., H/H_s = 1; α = 0.90.

	Value of $gp(\hat{y})/wH$								
$\hat{y} = y/H$	$R_w \leq .5$	R_w=.7	R_w=.8	R_w=.9	R_w=.95	R_w=1.0	R_w=1.05	R_w=1.1	R_w=1.2
1.00	0	0	0	0	0	0	0	0	0
0.95	.070	.073	.076	.082	.088	.089	.069	.064	.062
0.90	.112	.118	.124	.136	.149	.149	.110	.100	.095
0.85	.127	.135	.144	.162	.181	.181	.123	.108	.101
0.80	.133	.144	.155	.179	.204	.205	.127	.107	.098
0.75	.141	.154	.168	.197	.228	.229	.133	.108	.097
0.70	.145	.161	.177	.212	.249	.249	.135	.105	.092
0.65	.143	.161	.179	.219	.261	.262	.130	.096	.081
0.60	.139	.159	.179	.234	.271	.272	.124	.085	.067
0.55	.137	.159	.182	.231	.283	.283	.119	.076	.057
0.50	.135	.159	.183	.236	.293	.292	.114	.067	.046
0.45	.130	.155	.181	.238	.299	.298	.106	.055	.032
0.40	.124	.150	.178	.238	.303	.301	.097	.044	.019
0.35	.121	.148	.177	.241	.309	.307	.091	.035	.009
0.30	.118	.146	.177	.243	.313	.311	.086	.027	.000
0.25	.113	.142	.174	.242	.315	.312	.078	.017	.000
0.20	.109	.139	.171	.241	.316	.312	.071	.008	.000
0.15	.107	.137	.170	.242	.318	.313	.067	.003	.000
0.10	.106	.136	.170	.242	.320	.313	.064	.000	.000
0.05	.103	.134	.167	.241	.318	.311	.059	.000	.000
0	.101	.133	.166	.239	.317	.309	.056	.000	.000

Table A.4(c) Standard values for the hydrodynamic pressure function $p(\hat{y})$ for full reservoir, i.e., H/H_s = 1; α = 0.75.

	Value of $gp(\hat{y}) / wH$								
$\hat{y} = y / H$	$R_w \leq .5$	R_w=.7	R_w=.8	R_w=.9	R_w=.95	R_w=1.0	R_w=1.05	R_w=1.1	R_w=1.2
1.00	0	0	0	0	0	0	0	0	0
0.95	.070	.073	.075	.079	.080	.078	.073	.068	.065
0.90	.112	.118	.122	.129	.132	.128	.118	.101	.101
0.85	.127	.133	.140	.151	.154	.150	.134	.121	.110
0.80	.133	.143	.152	.166	.171	.163	.142	.125	.110
0.75	.140	.153	.164	.181	.187	.177	.151	.130	.110
0.70	.145	.159	.173	.193	.200	.188	.157	.131	.108
0.65	.143	.159	.174	.197	.205	.191	.155	.126	.099
0.60	.139	.157	.174	.199	.208	.192	.151	.118	.088
0.55	.137	.157	.175	.203	.213	.195	.150	.113	.079
0.50	.135	.156	.176	.206	.216	.196	.147	.107	.070
0.45	.129	.152	.173	.205	.216	.194	.140	.097	.058
0.40	.123	.147	.170	.203	.214	.191	.134	.088	.045
0.35	.120	.145	.169	.204	.215	.190	.129	.080	.036
0.30	.117	.143	.168	.204	.215	.188	.125	.074	.027
0.25	.112	.139	.164	.201	.212	.184	.118	.065	.016
0.20	.108	.135	.161	.199	.209	.180	.111	.056	.007
0.15	.106	.134	.159	.198	.208	.177	.107	.051	.001
0.10	.104	.133	.158	.197	.207	.175	.103	.046	.000
0.05	.102	.130	.156	.194	.204	.171	.098	.040	.000
0	.100	.128	.154	.192	.201	.167	.093	.036	.000

Table A.4(d) Standard values for the hydrodynamic pressure function $p(\hat{y})$ for full reservoir, i.e., H/H_s = 1; α = 0.50.

	Value of $gp(\hat{y}) / wH$								
$\hat{y} = y / H$	$R_w \leq .5$	R_w=.7	R_w=.8	R_w=.9	R_w=.95	R_w=1.0	R_w=1.05	R_w=1.1	R_w=1.2
1.00	0	0	0	0	0	0	0	0	0
0.95	.071	.072	.073	.074	.074	.073	.072	.070	.068
0.90	.112	.116	.118	.119	.119	.118	.116	.113	.108
0.85	.125	.132	.135	.136	.135	.134	.130	.127	.120
0.80	.132	.139	.143	.146	.145	.143	.138	.133	.123
0.75	.139	.148	.153	.156	.155	.152	.146	.139	.127
0.70	.144	.154	.160	.163	.162	.158	.151	.143	.128
0.65	.141	.152	.159	.163	.161	.156	.148	.138	.122
0.60	.137	.149	.157	.162	.160	.153	.143	.132	.113
0.55	.135	.148	.156	.161	.158	.151	.141	.128	.107
0.50	.133	.147	.155	.159	.156	.148	.137	.123	.099
0.45	.127	.142	.150	.154	.151	.142	.129	.115	.088
0.40	.121	.136	.145	.149	.145	.136	.122	.106	.077
0.35	.117	.133	.143	.146	.142	.131	.116	.099	.069
0.30	.114	.131	.140	.143	.137	.126	.110	.092	.060
0.25	.109	.126	.135	.137	.131	.119	.102	.083	.050
0.20	.104	.121	.130	.132	.125	.112	.094	.074	.040
0.15	.102	.119	.127	.128	.121	.108	.089	.068	.033
0.10	.100	.117	.125	.125	.118	.104	.083	.062	.026
0.05	.098	.114	.121	.121	.113	.098	.077	.055	.018
0	.096	.111	.119	.117	.108	.093	.072	.049	.012

Table A.4(e) Standard values for the hydrodynamic pressure function $p(\hat{y})$ for full reservoir, i.e., H/H_s = 1; α = 0.25.

	Value of $gp(\hat{y})/wH$								
$\hat{y} = y/H$	$R_w \leq .5$	R_w=.7	R_w=.8	R_w=.9	R_w=.95	R_w=1.0	R_w=1.05	R_w=1.1	R_w=1.2
1.00	0	0	0	0	0	0	0	0	0
0.95	.069	.070	.071	.071	.071	.071	.070	.070	.070
0.90	.111	.113	.114	.114	.114	.114	.113	.113	.111
0.85	.124	.127	.128	.129	.129	.128	.127	.127	.125
0.80	.130	.133	.134	.135	.135	.134	.133	.132	.129
0.75	.137	.141	.142	.143	.142	.141	.140	.138	.135
0.70	.141	.145	.147	.147	.146	.145	.143	.141	.137
0.65	.137	.142	.144	.144	.143	.142	.140	.137	.131
0.60	.133	.138	.140	.139	.138	.136	.134	.131	.124
0.55	.131	.136	.137	.136	.135	.133	.130	.126	.118
0.50	.128	.133	.134	.133	.131	.128	.125	.121	.112
0.45	.121	.126	.127	.126	.124	.120	.116	.112	.101
0.40	.115	.120	.120	.118	.115	.112	.107	.102	.091
0.35	.111	.116	.116	.113	.110	.106	.100	.095	.082
0.30	.107	.111	.111	.107	.104	.099	.093	.087	.074
0.25	.101	.105	.104	.100	.096	.091	.084	.077	.063
0.20	.096	.099	.098	.093	.088	.082	.076	.068	.052
0.15	.094	.096	.094	.088	.083	.076	.069	.061	.044
0.10	.092	.096	.090	.083	.078	.071	.063	.054	.037
0.05	.088	.088	.085	.077	.071	.064	.055	.046	.028
0	.086	.085	.081	.072	.065	.057	.048	.039	.020

Table A.4(f) **Standard values for the hydrodynamic pressure function $p(\hat{y})$ for full reservoir, i.e., H/H_s = 1; α = 0.**

	Value of $gp(\hat{y}) / wH$								
$\hat{y} = y / H$	$R_w \leq .5$	R_w=.7	R_w=.8	R_w=.9	R_w=.95	R_w=1.0	R_w=1.05	R_w=1.1	R_w=1.2
1.00	0	0	0	0	0	0	0	0	0
0.95	.069	.069	.069	.069	.069	.069	.070	.070	.070
0.90	.109	.110	.110	.111	.111	.111	.112	.112	.112
0.85	.122	.123	.124	.125	.125	.125	.126	.126	.126
0.80	.127	.128	.128	.129	.129	.129	.130	.130	.130
0.75	.133	.134	.134	.135	.135	.135	.136	.136	.136
0.70	.135	.136	.137	.138	.138	.138	.139	.139	.139
0.65	.132	.133	.133	.133	.133	.133	.134	.134	.134
0.60	.127	.127	.127	.127	.127	.127	.127	.127	.127
0.55	.123	.123	.123	.123	.123	.123	.122	.122	.121
0.50	.120	.119	.118	.118	.118	.117	.116	.116	.115
0.45	.113	.111	.110	.109	.109	.108	.107	.106	.105
0.40	.105	.103	.102	.100	.099	.098	.097	.096	.094
0.35	.101	.098	.096	.094	.092	.091	.090	.088	.085
0.30	.096	.092	.090	.087	.085	.084	.082	.080	.076
0.25	.090	.085	.082	.078	.076	.074	.072	.069	.065
0.20	.084	.078	.074	.070	.067	.065	.062	.059	.053
0.15	.080	.073	.068	.064	.061	.058	.055	.051	.045
0.10	.077	.069	.064	.058	.054	.051	.048	.044	.036
0.05	.073	.063	.057	.050	.046	.043	.039	.035	.026
0	.070	.058	.052	.044	.040	.036	.031	.027	.017

Table A.5(a) Standard values for A_p, the hydrodynamic force coefficient in $\tilde{L}_1$; α = 1.0.

R_w	Value of A_p for α=1
0.99	1.242
0.98	.893
0.97	.739
0.96	.647
0.95	.585
0.94	.539
0.93	.503
0.92	.474
0.90	.431
0.85	.364
0.80	.324
0.70	.279
≤ 0.50	.237

Table A.5(b) Standard values for A_p, the hydrodynamic force coefficient in $\tilde{L}_1$; α = 0.90, 0.75, 0.50, 0.25 and 0.

	Value of A_p				
R_w	α=0.90	α=0.75	α=0.50	α=0.25	α=0
1.20	.071	.111	.159	.178	.181
1.10	.110	.177	.204	.197	.186
1.05	.194	.249	.229	.205	.189
1.00	.515	.340	.252	.213	.191
0.95	.518	.378	.267	.219	.193
0.90	.417	.361	.274	.224	.195
0.80	.322	.309	.269	.229	.198
0.70	.278	.274	.256	.228	.201
≤ 0.50	.237	.236	.231	.222	.206

Table A.6 Standard values for the hydrodynamic pressure function $p_0(\hat{y})$.

$\hat{y} = y / H$	gp_0 / wH
1.0	0
0.95	.137
0.90	.224
0.85	.301
0.80	.362
0.75	.418
0.70	.465
0.65	.509
0.60	.546
0.55	.580
0.50	.610
0.45	.637
0.40	.659
0.35	.680
0.30	.696
0.25	.711
0.20	.722
0.15	.731
0.10	.737
0.05	.741
0	.742

Appendix B Probabilistic Seismic Hazard Analysis for Pine Flat Dam Site

Summarized in this appendix is the probabilistic seismic hazard analysis (PSHA) performed for the Pine Flat Dam site to obtain the ensemble of ground motions used in the response analysis presented in Chapter 6.

B.1 TARGET SPECTRUM

Figure B.1 shows two Conditional Mean Spectra (CMS) for the Pine Flat Dam site computed by the procedure in Baker [2011] at the 1% in 100 years hazard level for the intensity measures $A(T_1)$ and $A(\tilde{T}_1)$, where $T_1 \approx 0.3$ sec and $\tilde{T}_1 \approx 0.5$ sec are the fundamental vibration periods of the dam alone on a rigid foundation and the dam with impounded water on flexible foundation, respectively. These values cover the range of periods for the four analysis cases listed in Table 6.1.

It was decided to evaluate the accuracy of the RSA procedure using the same ensemble of ground motions for all the four analysis cases considered; thus ground motions were selected and scaled for a single target spectrum. Because the two CMS corresponding to the periods T_1 and $\tilde{T}_1$ are very similar, the target spectrum is, for convenience, taken as the geometric mean of the two CMS, shown in Figure B.1. Although more rigorous procedures exist for computing CMS for an intensity measure that averages spectral acceleration values over a range of periods [Baker and Cornell 2006], the target spectrum selected is considered satisfactory for the limited objective of comparing the RSA and RHA procedures.

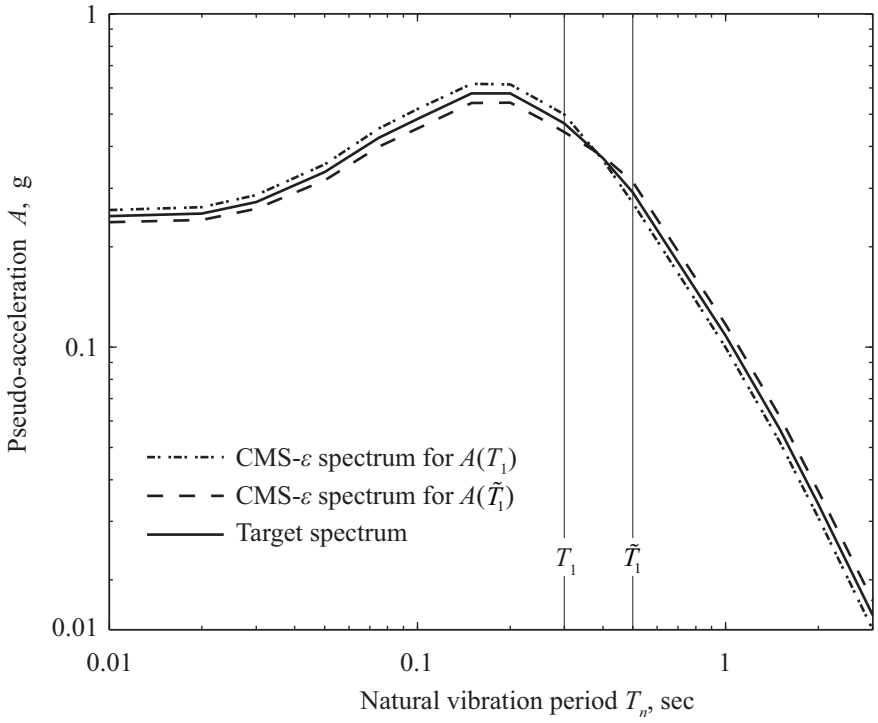

Figure B.1 CMS-ε spectra for intensity measures $A(T_1)$ and $A(\tilde{T}_1)$ at the 1% in 100 years hazard level. Also plotted is the target spectrum; damping, ζ = 5%.

B.2 SELECTION AND SCALING OF GROUND MOTIONS

The 29 acceleration records listed in Table B.1, each with two orthogonal horizontal components, were selected from the PEER Ground Motion Database [PEER Ground Motion 2010] according to the following criteria:

- Fault distance, R = 0–50 km
- Magnitude, M_w = 5–7.5
- Shear wave velocity, $V_{s,30}$ > 183 m/sec (corresponding to minimum NEHRP soil class D, stiff soil).

The range of M_w and R were selected to be consistent with the deaggregation of the seismic hazard at the Pine Flat Dam site [USGS Deaggregation 2008] where it was clear that the dominant events at the site for the main periods of interest were close distance earthquakes in magnitude range M_w = 5 - 7.5. The range of $V_{s,30}$ was chosen to discard ground motions recorded on very soft soils, which are not representative for the rock site at Pine Flat Dam.

The selected records were amplitude-scaled by scaling each ground motion to minimize the mean square difference between the response spectrum for the individual ground motion and

the target spectrum over the period range of interest. A detailed description of this scaling procedure can be found in PEER Ground Motion [2010].

Figure B.2 presents the response spectra for the scaled ground motions, the target spectrum, and the median (computed as the geometric mean) of the 58 response spectra.

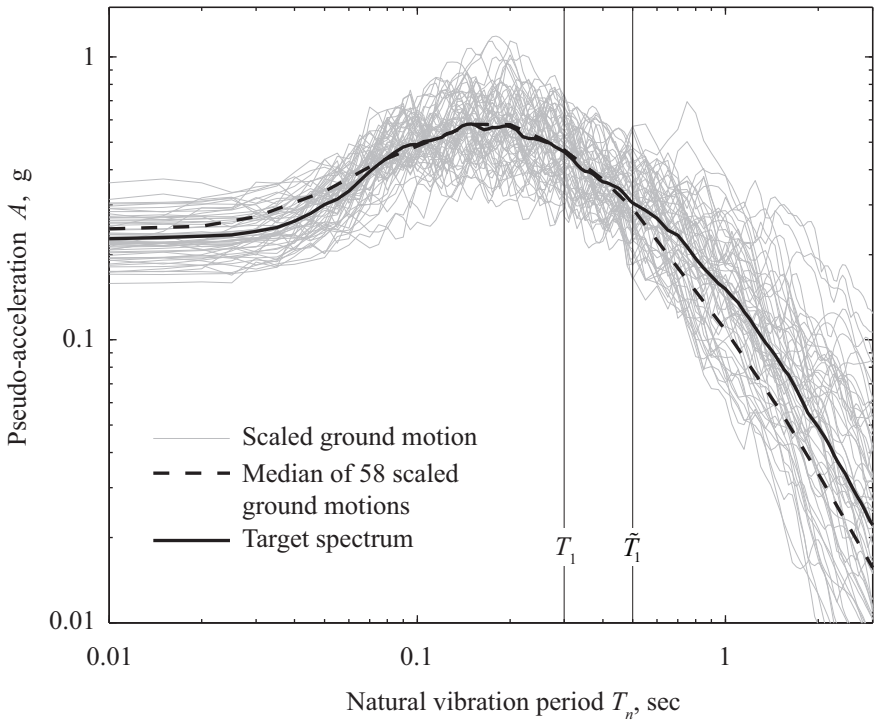

Figure B.2 Response spectra for 58 scaled ground motion records, their median spectrum, and the target spectrum; damping, ζ = 5%.

Table B.1 List of earthquake records. PGA values are for the scaled fault-normal and fault-parallel components of the ground motions.

#	Year	Event	Station	M_w	R, in km.	PGA, in g	
						FN comp.	FP comp.
1	1966	Parkfield	Cholame Shandon Array	6.19	17.6	0.232	0.246
2	1971	San Fernando	LA - Hollywood Stor FF	6.61	22.8	0.180	0.229
3	1971	San Fernando	Lake Hughes 4	6.61	25.1	0.256	0.319
4	1979	Imperial Valley	Victoria	6.53	31.9	0.179	0.306
5	1980	Mammoth Lakes	Mammoth Lakes H.S.	6.06	4.7	0.179	0.271
6	1980	Irpinia, Italy	Auletta	6.90	9.5	0.198	0.211
7	1980	Irpinia, Italy	Rionero In Vulture	6.90	30.1	0.226	0.210
8	1983	Mammoth Lakes	Convict Creek	5.31	7.1	0.191	0.313
9	1983	Coalinga 05	Oil Fields Fire Station FF	5.77	11.1	0.292	0.243
10	1984	Morgan Hill	Gilroy Array #2	6.19	13.7	0.278	0.228
11	1986	N. Palm Springs	San Jacinto - Valley Cemetary	6.06	31.0	0.253	0.219
12	1986	N. Palm Springs	Sunnymead	6.06	37.9	0.236	0.227
13	1986	Chalfant Valley	Benton	6.19	21.9	0.251	0.214
14	1987	Whittier Narrows	Glendale - Las Palmas	5.99	22.8	0.312	0.189
15	1987	Whittier Narrows	Glendora - N. Oakbank	5.99	22.1	0.282	0.205
16	1987	Whittier Narrows	LA - Century City CC North	5.99	29.9	0.188	0.275
17	1987	Whittier Narrows	Pomona - 4th&Locust FF	5.99	29.6	0.262	0.224
18	1987	Whittier Narrows	LA - Hollywood Stor FF	5.27	24.8	0.200	0.278
19	1992	Landers	Mission Creek Fault	7.28	27.0	0.223	0.231
20	1994	Northridge	Burbank - Howard Rd	6.69	16.9	0.134	0.171
21	1994	Northridge	LA - Centinela St	6.69	28.3	0.198	0.300
22	1994	Northridge	LA - Obregon Park	6.69	37.4	0.370	0.197
23	1994	Northridge	LA - Wonderland Ave	6.69	20.3	0.243	0.183
24	1994	Northridge	Santa Monica City Hall	6.69	26.4	0.216	0.324
25	1999	Hector Mine	Twentynine Palms	7.13	42.1	0.215	0.220
26	1999	Chi-Chi, Taiwan	TCU079	6.20	8.5	0.260	0.200
27	1999	Chi-Chi, Taiwan	TCU054	6.20	49.5	0.210	0.266
28	1999	Chi-Chi, Taiwan	TCU075	6.30	26.3	0.300	0.163
29	1999	Chi-Chi, Taiwan	TCU120	6.30	32.5	0.243	0.221

Appendix C Detailed Calculations for Pine Flat Dam

This appendix presents detailed calculations of the equivalent lateral earthquake forces and earthquake induced stresses in Pine Flat Dam that were presented in Chapter 6. The appendix consists of two parts: (1) a summary of the computational steps required in the RSA procedure; and (2) a brief summary of the procedure for obtaining stresses in the RHA procedure using a newer version of the computer program EAGD-84.

C.1 RESPONSE SPECTRUM ANALYSIS PROCEDURE

The dam is analyzed for the four analysis cases listed in Table C.2. For each case the equivalent static lateral forces are computed by implementing the step-by-step procedure presented in Chapter 4, and stresses are computed using the methods described in the subsequent sections. All computations are performed for a unit width of the dam monolith.

Simplified Block Model of Dam Monolith

The simplified model of the tallest, non-overflow cross-section of Pine Flat Dam is shown in Figure C.1. The cross-section is divided into 10 blocks of equal height of 40 ft, the properties of each of the blocks are presented in Table C.1. The total weight of the dam in the simplified block model is 9486 kips, and the modal parameters L_1 and M_1 are computed by replacing the integrals in Equations (2.4) and (2.5) by their respective summations over all the blocks, which yields L_1 = (1390 kips) / g and M_1 = (500 kips) / g.

Table C.1 Properties of each block in the simplified model.

Block	Weight, w, kips	Elevation of centroid, ft.	ϕ_1 at centroid	$w\phi_1$, kips	$w\phi_1^2$, kips
1	202.8	379.9	0.865	175.4	151.8
2	267.3	338.5	0.612	163.7	100.2
3	417.7	298.6	0.450	188.1	84.7
4	610.8	258.9	0.331	202.3	67.0
5	816.7	219.2	0.238	194.6	46.4
6	1022.5	179.3	0.164	167.7	27.5
7	1228.3	139.4	0.107	131.8	14.2
8	1434.2	99.5	0.065	92.6	6.0
9	1640.0	59.6	0.034	55.3	1.9
10	1845.9	19.6	0.010	18.1	0.2
Total	9486			1390	500

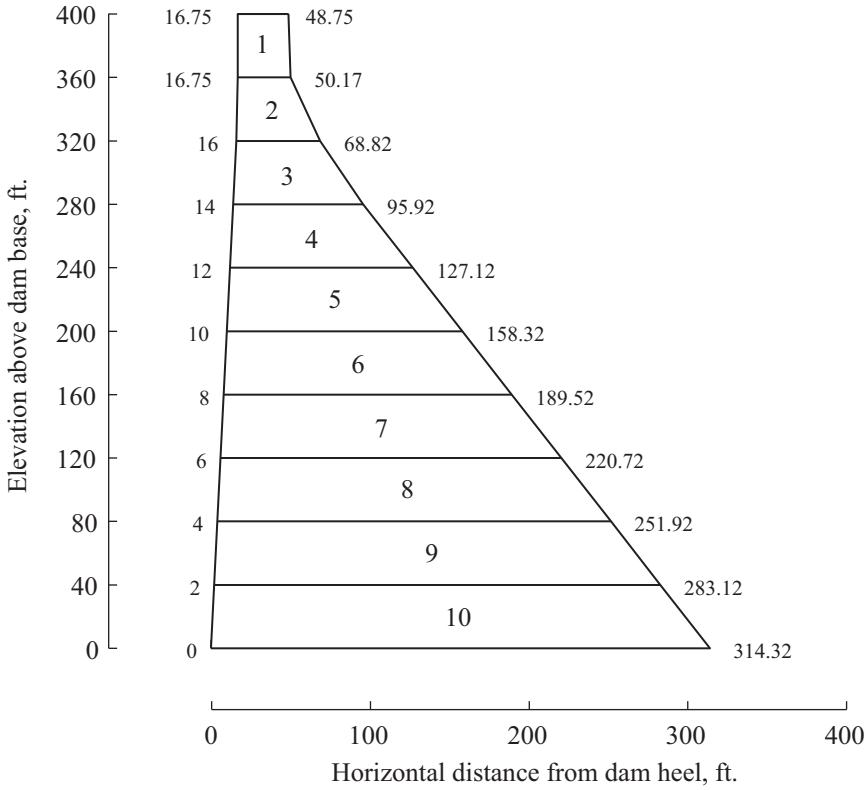

Figure C.1 Coordinates of simplified block model.

Computation of Equivalent Static Lateral Forces

The equivalent static lateral forces associated with the fundamental mode, f_1, and higher modes, f_{sc}, are computed by implementing the step-by-step procedure described in Chapter 4. The details of the computational steps are summarized in this section.

1. For $E_s = 3.25$ million psi and $H_s = 400$ ft., T_1 is computed from Equation (3.1) as $T_1 = (1.4)(400)/\sqrt{3.25 \cdot 10^6} = 0.311$ sec.

2. For $E_s = 3.25$ million psi, $\alpha = 0.75$ and $H/H_s = 381/400 = 0.95$, Table A.2(b) gives $R_r = 1.246$ (linearly interpolated between values for $E_s = 3.0$ million psi and $E_s = 3.5$ million psi), so $\tilde{T}_r = (1.240)(0.311) = 0.387$ sec.

3. The fundamental vibration period for the impounded water is $T_1^r = 4H/C = 4(381)/4720 = 0.323$ sec, Equation (3.2) then gives $R_w = 0.323/0.387 = 0.83$.

4. For $E_f/E_s = 1$, Table A.3 gives $R_f = 1.187$, leading to $\tilde{T}_1 = (1.187)(0.311) = 0.369$ sec for Case 3, and $\tilde{T}_1 = (1.187)(0.387) = 0.459$ sec for Case 4.

5. For Cases 2 and 4, Table A.2(b) gives $\zeta_r = 0.023$ for $E_s = 3.25$ million psi (interpolated), $\alpha = 0.75$, and $H/H_s = 0.95$. For Cases 3 and 4, $\zeta_f = 0.059$ from Table A.3 for $E_f/E_s = 1$ and $\eta_f = 0.04$. With $\zeta_1 = 0.02$, Equation (2.9) then gives: $\tilde{\zeta}_1 = 0.02/1.246 + 0.023 = 0.039$ for Case 2; $\tilde{\zeta}_1 = 0.02/(1.187)^3 + 0.059 = 0.071$ for Case 3; and $\tilde{\zeta}_1 = 0.02/[(1.24)(1.187)^3] + 0.023 + 0.059 = 0.092$ for Case 4.

6. The values of $gp(y)$ presented in Table C.3 at eleven equally spaced levels were obtained from Table A.4(c) for $R_w = 0.83$ (by linearly interpolating between the data for the two closest values for which data are available, $R_w = 0.80$ and $R_w = 0.90$) and $\alpha = 0.75$, and multiplied by (0.0624)(381)(.95)^2 = 21.6 k/ft.

7. Evaluating Equation (2.4) in discrete form gives $M_1 = (500\,\text{kip})/g$. From Equation (3.3), $\tilde{M}_1 = (1.246)^2(1/g)(500) = (776\,\text{kip})/g$.

8. Evaluating Equation (2.5) in discrete form gives $L_1 = (1390\,\text{kip})/g$. From Table A.5(b), $A_p = 0.327$ for $\alpha = 0.75$ and $R_w = 0.83$ (interpolated). Equation (3.4) then gives $\tilde{L}_1 = 1390/g + (1/g)(4529)(0.95)^2(0.327) = (2732\,\text{kip})/g$. Consequently, for Cases 1 and 3, $\tilde{\Gamma}_1 = L_1/M_1 = 1390/500 = 2.78$, and for Cases 2 and 4, $\tilde{\Gamma}_1 = \tilde{L}_1/\tilde{M}_1 = 2732/776 = 3.52$.

9. For each of the four cases listed in Table C.2, Equation (2.1) was evaluated at eleven equally spaced intervals along the height of the dam, including the top and bottom, by substituting values for $\tilde{\Gamma}_1 = \tilde{L}_1/\tilde{M}_1$ and $gp(y)$ computed in the preceding steps; computing the weight of the dam per unit height $w_s(y)$ from the monolith dimensions shown in Figure C.1 and the unit weight of concrete; and substituting $\phi_1(y)$ from Table A.1 and the pseudo-acceleration ordinate $A(\tilde{T}_1, \tilde{\zeta}_1)$ from the median pseudo-acceleration response spectrum in Figure 6.2 corresponding to the $\tilde{T}_1$ and $\tilde{\zeta}_1$ computed in Steps 4 and

5. The resulting equivalent static lateral forces $f_1(y)$ are presented in Table C.4 for each case, with intermediate values shown in Table C.3.

10. The vertical stresses $\sigma_{y,1}$ due to the response of the dam in its fundamental mode are computed by a static stress analysis of the dam subjected to the equivalent static lateral forces $f_1(y)$ from Step 9 applied to the upstream face of the dam. A summary of the static stress analysis is presented in the next subsection.

11. For each of the four cases, Equation (2.10) was evaluated at eleven equally spaced intervals along the height of the dam, including the top and bottom, by substituting numerical values for the quantities computed in the preceding steps; obtaining $gp_0(y)$ from Table A.6; using Equation (2.11) to compute $B_1 = (0.20)(4529/g)(0.95)^2 = (817.5\text{kip})/g$, which yields $B_1/M_1 = 817.5/500 = 1.64$; and substituting $a_g = 0.232$ g. The resulting equivalent static lateral forces $f_{sc}(y)$ are presented in Table C.4 for each case, with intermediate values shown in Table C.3.

12. The vertical stresses $\sigma_{y,sc}$ due to the response of the dam in all higher modes are computed by a static stress analysis of the dam subjected to the equivalent static lateral forces $f_{sc}(y)$ from Step 11 applied to the upstream face of the dam. A summary of the static stress analysis is presented in the next subsection.

13. Computation of the earthquake induced vertical stresses $\sigma_{y,d}$ is done by combining the response quantities $\sigma_{y,1}$ and $\sigma_{y,sc}$ computed in Steps 10 and 12 by the SRSS combination rule; this is described in a later subsection.

Table C.2 Analysis cases, fundamental mode properties and pseudo-acceleration values.

Analysis Case	Foundation	Water	$\tilde{\Gamma}_1 = \tilde{L}_1/\tilde{M}_1$	$\tilde{T}_1$, in sec	$\tilde{\zeta}_1$, in percent	$A(\tilde{T}_1, \tilde{\zeta}_1)$, in g
1	Rigid	Empty	2.78	0.311	2.0	0.606
2	Rigid	Full	3.52	0.387	3.9	0.409
3	Flexible	Empty	2.78	0.369	7.1	0.347
4	Flexible	Full	3.52	0.459	9.2	0.274

Table C.3 Intermediate values for calculation of equivalent static lateral forces.

y, ft.	w_s, k/ft.	ϕ_1	$w_s\phi_1$, k/ft.	$w_s[1-(L_1/M_1)\phi_1]$, k/ft.	gp, k/ft.	gp_0 k/ft.	$gp_0-(B_1/M_1)w_s\phi_1$, k/ft.
400	4.96	1.000	4.96	-8.83	0	0	-8.16
360	5.18	0.735	3.81	-5.41	1.75	3.47	-2.79
320	8.19	0.530	4.34	-3.88	3.16	7.45	0.31
280	12.7	0.389	4.94	-1.04	3.73	10.3	2.15
240	17.8	0.284	5.07	3.75	3.94	12.5	4.12
200	23.0	0.200	4.60	10.20	3.99	14.1	6.59
160	28.1	0.135	3.80	17.57	3.94	15.6	9.21
120	33.3	0.084	2.80	25.51	3.87	16.4	11.8
80	38.4	0.047	1.81	33.41	3.76	17.1	14.1
40	43.6	0.021	0.92	41.03	3.69	17.5	16.0
0	48.7	0	0	48.72	3.60	17.6	17.6

Table C.4 Equivalent static lateral forces in kips/ft on Pine Flat Dam.

y, ft.	Case 1		Case 2		Case 3		Case 4	
	f_1	f_{sc}	f_1	f_{sc}	f_1	f_{sc}	f_1	f_{sc}
400	8.31	- 2.05	7.02	- 3.94	4.74	- 2.05	4.78	- 3.94
360	6.38	- 1.25	7.86	- 1.90	3.64	- 1.25	5.36	- 1.90
320	7.27	- 0.90	10.6	- 0.83	4.15	- 0.90	7.24	- 0.83
280	8.28	- 0.24	12.3	0.26	4.72	- 0.24	8.36	0.26
240	8.49	0.87	12.8	1.83	4.85	0.87	8.69	1.83
200	7.71	2.37	12.2	3.90	4.40	2.37	8.28	3.90
160	6.37	4.08	11.0	6.21	3.63	4.08	7.47	6.21
120	4.69	5.92	9.44	8.66	2.67	5.92	6.43	8.66
80	3.03	7.75	7.88	11.0	1.73	7.75	5.37	11.0
40	1.53	9.52	6.52	13.2	0.88	9.52	4.44	13.2
0	0.00	11.3	5.10	15.4	0.00	11.3	3.47	15.4

Computation of Vertical Stresses

The vertical stresses $\sigma_{y,1}$ and $\sigma_{y,sc}$ due to each set of equivalent static lateral forces $f_1(y)$ and $f_{sc}(y)$, respectively, are computed by static stress analysis of the dam monolith by two different methods: (1) stresses at both faces of the dam are computed by elementary formulas for stresses in beams; and (2) stresses are computed by a finite element analysis.

Results are presented in this section for analysis case 4 only, as the computational steps are identical for all the four analysis cases.

Beam Theory

The inertia forces associated with the mass—given by the first term of Equations (2.1) and (2.10)—are applied at the centroid of each of the 10 blocks shown in Figure C.1, and the forces associated with hydrodynamic pressure—given by the second term of the same equations—are applied as a linearly distributed load on the upstream face of each block. The resulting bending moments in the dam monolith are computed at each level from the equilibrium equations, and the normal bending stresses at two faces are computed by elementary beam theory as $\sigma_y = M / S$, where M and S are the bending moment and section modulus, respectively, at the horizontal section considered; these stresses act in the vertical direction. The procedure is implemented in a newly developed computer program similar to the computer program SIMPL described in Appendix D of Fenves and Chopra [1986]. The vertical stresses computed at the two faces of Pine Flat Dam are listed in Table C.5 for analysis case 4.

The stresses with their algebraic signs shown in Table C.5 will occur on the upstream face of the dam when the earthquake forces act in the downstream direction, and on the downstream face of the dam when the earthquake forces act in the upstream direction. The stresses on the sloping part of the downstream face are subsequently multiplied by the correction factor of 0.75 developed in Section 4.3.

Table C.5 Vertical stresses $\sigma_{y,1}$ and $\sigma_{y,sc}$ for analysis case 4 computed by elementary beam theory.

		Fundamental mode		Higher modes	
y, ft.	Section modulus, $S = 1/6b^2$, ft^3	Bending moment, k-ft.	Vertical stress at faces, psi	Bending moment, k-ft.	Vertical stress at faces, psi
400	171	0	0	0	0
360	186	3,479	130	-2,579	-96
320	465	15,577	233	-8,632	-129
280	1,118	39,103	243	-16,060	-100
240	2,208	75,854	239	-23,020	-72
200	3,665	126,35	239	-26,978	-51
160	5,490	190,037	240	-24,673	-31
120	7,683	265,64	240	-12,398	-11
80	10,242	351,517	238	13,675	9
40	13,170	446,139	235	57,289	30
0	16,464	547,841	231	122,028	51

Finite Element Method

The forces $f_1(y)$ and $f_{sc}(y)$ are applied as linearly distributed forces to the upstream face of the finite element discretization of the dam shown in Figure C.2. Static analysis of the finite element model leads to stresses at the centroid of each element, and a stress recovery procedure is applied in order to obtain stresses at the nodal points.

The resulting vertical stresses $\sigma_{y,1}$ and $\sigma_{y,sc}$, at the nodal points on the two faces of the dam due to earthquake forces applied in the downstream direction are listed in Table C.6 for analysis case 4. Applying the forces in the upstream direction reverses the algebraic signs of the stresses; numerical values remain unchanged.

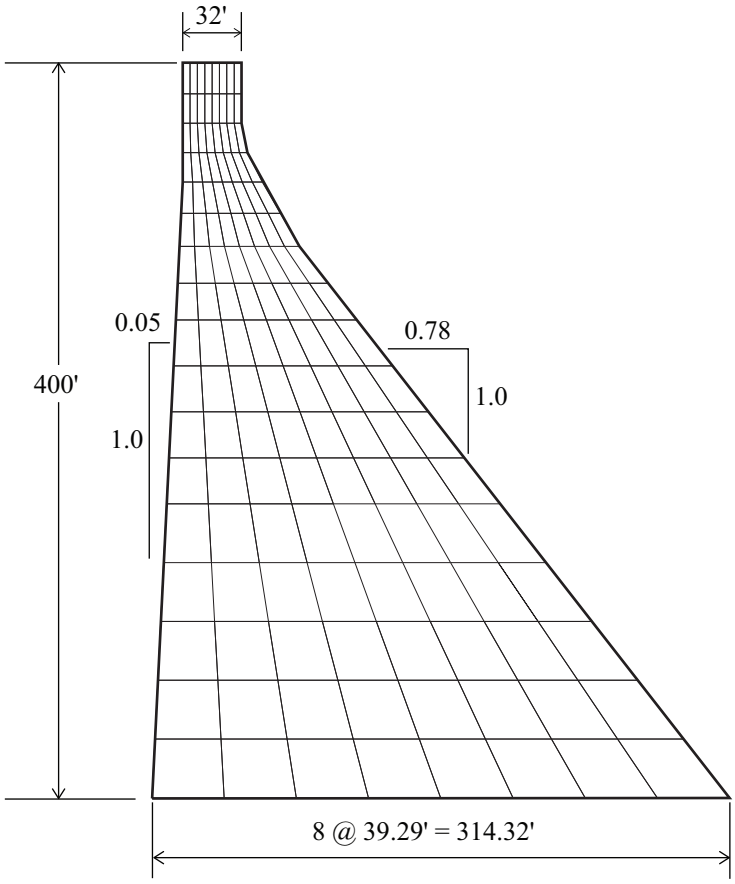

Figure C.2 **Finite element model of Pine Flat Dam used for stress computations in the RSA procedure; mesh consists of 136 quadrilateral four-node elements. The same mesh is used in the RHA procedure.**

Table C.6 **Vertical stresses $\sigma_{y,1}$ and $\sigma_{y,sc}$, in psi, for analysis case 4 computed by finite element analysis.**

	Fundamental mode		Higher modes	
Height, y, ft.	Vertical stress at u/s face	Vertical stress at d/s face	Vertical stress at u/s face	Vertical stress at d/s face
400	12	-9	-9	7
383	34	-34	-24	25
367	92	-108	-61	71
351	160	-183	-98	110
335	209	-207	-118	111
318	232	-214	-119	100
300	240	-216	-110	88
280	243	-200	-98	69
260	241	-190	-86	54
235	239	-190	-73	42
210	237	-190	-62	30
185	237	-190	-52	18
160	238	-185	-43	4
128	241	-176	-32	-9
96	249	-161	-19	-19
64	264	-140	3	-26
32	290	-118	44	-27
0	306	-107	71	-27

Response Combination

The vertical stress at a location due to earthquake excitation is computed by combining $\sigma_{y,1}$ and $\sigma_{y,sc}$ by the SRSS formula:

$$\sigma_{y,d} = \pm\sqrt{\sigma_{y,1}^2 + \sigma_{y,sc}^2} \tag{C.1}$$

Because the direction of the applied earthquake forces is reversible, these stresses can be either positive (tensile stresses) or negative (compressive stresses).

The earthquake induced vertical stresses for Pine Flat Dam computed by beam theory and the finite element method are summarized in Tables C.7 and C.8 for analysis case 4; stresses computed by beam theory on the sloping part of the downstream face have been modified by the correction factor of 0.75. These results are also presented in Section 6.3.2.

Table C.7 **Vertical stresses $\sigma_{y,d}$, in psi, for analysis case 4 computed by beam theory.**

Height, y, ft.	Vertical stress at u/s face	Vertical stress at d/s face
400	0	0
360	162	162
320	266	200
280	263	197
240	250	187
200	245	184
160	242	182
120	240	180
80	239	179
40	237	179
0	237	178

Table C.8 **Vertical stresses $\sigma_{y,d}$, in psi, for analysis case 4 computed by finite element analysis.**

Height, y, ft.	Vertical stress at u/s face	Vertical stress at d/s face
400	15	12
383	42	42
367	110	130
351	188	213
335	240	234
318	261	236
300	264	234
280	262	212
260	256	197
235	250	195
210	245	192
185	242	190
160	242	185
128	244	176
96	250	162
64	264	143
32	294	121
0	314	110

Principal Stresses: Beam Theory

At the upstream and downstream faces of the dam, principal stresses due to each of the force distributions f_1 and f_{sc} can be determined by a simple transformation of the corresponding vertical stresses determined by beam theory. If the upstream face of the dam is nearly vertical and the effects of tail-water are negligible, this transformation can be written as [Fenves and Chopra 1986: Appendix C]

$$\sigma_1 = \sigma_{y,1} \sec^2 \theta \tag{C.2a}$$

$$\sigma_{sc} = \sigma_{y,sc} \sec^2 \theta \tag{C.2b}$$

where θ is the angle of the face with respect to the vertical. Under these restricted conditions the principal stresses are directly proportional to the vertical stresses, and hence also to the modal coordinate, therefore modal combination rules are applicable.

The maximum principal stresses on the two faces of the dam computed by combining σ_1 and σ_{sc} using the SRSS formula are shown in Table C.9, where the vertical stresses entering the Equation (C.2) are computed by beam theory. These values are also presented in Section 6.4.2, where they are compared to the results obtained by the RHA procedure.

Table C.9 **Maximum principal stresses σ_d, in psi, for analysis case 4 computed by beam theory.**

Height, y, ft	Maximum principal stress at u/s face	Maximum principal stress at d/s face
400	0	0
360	162	121
320	266	243
280	263	287
240	250	301
200	245	295
160	243	292
120	241	290
80	239	288
40	238	286
0	237	286

C.2 RESPONSE HISTORY ANALYSIS PROCEDURE

A set of pre- and post-processor scripts were developed to facilitate response history analyses for the 58 ground motions in the computer program EAGD-84 [Fenves and Chopra 1984c], this program provides stresses as a function of time for every element in the finite element model (mesh shown in Figure C.2). From the stress response histories the peak values of the maximum principal stress over the duration of each ground motion are determined, and the median value at every nodal point on the two faces is computed as the geometric mean of the stress values due to the 58 ground motions.

Such results are presented in Figure C.3 for the four analysis cases; the median results are also presented in Section 6.4.2 where they are compared with stresses computed by the RSA procedure.

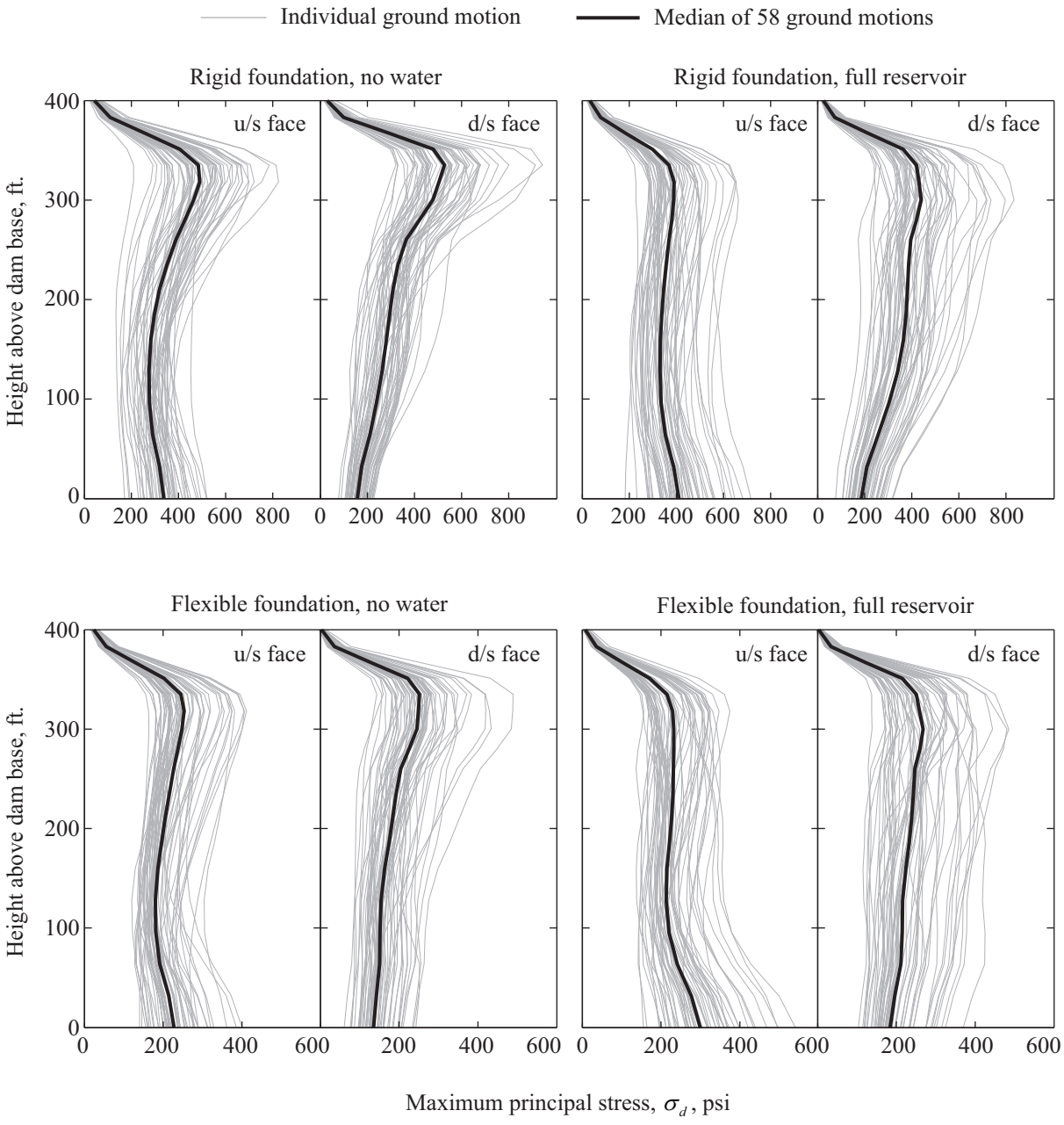

Figure C.3 **Peak maximum principal stresses, σ_d, at the two faces of Pine Flat Dam due to each of the 58 ground motions computed by RHA. Also plotted are the median values.**

PEER REPORTS

PEER reports are available as a free PDF download from http://peer.berkeley.edu/publications/peer_reports_complete.html. Printed hard copies of PEER reports can be ordered directly from our printer by following the instructions at http://peer.berkeley.edu/publications/peer_reports.html. For other related questions about the PEER Report Series, contact the Pacific Earthquake Engineering Research Center, 325 Davis Hall mail code 1792, Berkeley, CA 94720. Tel.: (510) 642-3437; Fax: (510) 665-1655; Email: peer_editor@berkeley.edu

PEER 2013/17 *Response Spectrum Analysis of Concrete Gravity Dams Including Dam-Water-Foundation Interaction.* Arnkjell Løkke and Anil K. Chopra. July 2013.

PEER 2013/16 *Effect of hoop reinforcement spacing on the cyclic response of large reinforced concrete special moment frame beams.* Marios Panagiotou, Tea Visnjic, Grigorios Antonellis, Panagiotis Galanis, and Jack P. Moehle. June 2013.

PEER 2013/15 *publication pending*

PEER 2013/14 *publication pending*

PEER 2013/13 *publication pending*

PEER 2013/12 *Nonlinear Horizontal Site Response for the NGA-West2 Project.* Ronnie Kamai, Norman A. Abramson, Walter J. Silva. May 2013.

PEER 2013/11 *Epistemic Uncertainty for NGA-West2 Models.* Linda Al Atik and Robert R. Youngs. May 2013.

PEER 2013/10 *NGA-West 2 Models for Ground-Motion Directionality.* Shrey K. Shahi and Jack W. Baker. May 2013.

PEER 2013/09 *Final Report of the NGA-West2 Directivity Working Group.* Paul Spudich, Jeffrey R. Bayless, Jack W. Baker, Brian S.J. Chiou, Badie Rowshandel, Shrey Shahi, and Paul Somerville. May 2013.

PEER 2013/08 *NGA-West2 Model for Estimating Average Horizontal Values of Pseudo-Absolute Spectral Accelerations Generated by Crustal Earthquakes.* I. M. Idriss. May 2013.

PEER 2013/07 *Update of the Chiou and Youngs NGA Ground Motion Model for Average Horizontal Component of Peak Ground Motion and Response Spectra.* Brian Chiou and Robert Youngs. May 2013.

PEER 2013/06 *NGA-West2 Campbell-Bozorgnia Ground Motion Model for the Horizontal Components of PGA, PGV, and 5%-Damped Elastic Pseudo-Acceleration Response Spectra for Periods Ranging from 0.01 to 10 sec.* Kenneth W. Campbell and Yousef Bozorgnia. May 2013.

PEER 2013/05 *NGA-West 2 Equations for Predicting Response Spectral Accelerations for Shallow Crustal Earthquakes.* David M. Boore, Jonathan P. Stewart, Emel Seyhan, Gail M. Atkinson. May 2013.

PEER 2013/04 *Update of the AS08 Ground-Motion Prediction Equations Based on the NGA-West2 Data Set.* Norman Abrahamson, Walter Silva, and Ronnie Kamai. May 2013.

PEER 2013/03 *PEER NGA-West2 Database.* Timothy D. Ancheta, Robert B. Darragh, Jonathan P. Stewart, Emel Seyhan, Walter J. Silva, Brian S.J. Chiou, Katie E. Wooddell, Robert W. Graves, Albert R. Kottke, David M. Boore, Tadahiro Kishida, and Jennifer L. Donahue. May 2013.

PEER 2013/02 *Hybrid Simulation of the Seismic Response of Squat Reinforced Concrete Shear Walls.* Catherine A. Whyte and Bozidar Stojadinovic. May 2013.

PEER 2013/01 *Housing Recovery in Chile: A Qualitative Mid-program Review.* Mary C. Comerio. February 2013.

PEER 2012/08 *Guidelines for Estimation of Shear Wave Velocity.* Bernard R. Wair, Jason T. DeJong, and Thomas Shantz. December 2012.

PEER 2012/07 *Earthquake Engineering for Resilient Communities: 2012 PEER Internship Program Research Report Collection.* Heidi Tremayne (Editor), Stephen A. Mahin (Editor), Collin Anderson, Dustin Cook, Michael Erceg, Carlos Esparza, Jose Jimenez, Dorian Krausz, Andrew Lo, Stephanie Lopez, Nicole McCurdy, Paul Shipman, Alexander Strum, Eduardo Vega. December 2012.

PEER 2012/06 *Fragilities for Precarious Rocks at Yucca Mountain.* Matthew D. Purvance, Rasool Anooshehpoor, and James N. Brune. December 2012.

PEER 2012/05 *Development of Simplified Analysis Procedure for Piles in Laterally Spreading Layered Soils.* Christopher R. McGann, Pedro Arduino, and Peter Mackenzie–Helnwein. December 2012.

PEER 2012/04 *Unbonded Pre-Tensioned Columns for Bridges in Seismic Regions.* Phillip M. Davis, Todd M. Janes, Marc O. Eberhard, and John F. Stanton. December 2012.

PEER 2012/03 *Experimental and Analytical Studies on Reinforced Concrete Buildings with Seismically Vulnerable Beam-Column Joints.* Sangjoon Park and Khalid M. Mosalam. October 2012.

PEER 2012/02 *Seismic Performance of Reinforced Concrete Bridges Allowed to Uplift during Multi-Directional Excitation.* Andres Oscar Espinoza and Stephen A. Mahin. July 2012.

PEER 2012/01 *Spectral Damping Scaling Factors for Shallow Crustal Earthquakes in Active Tectonic Regions.* Sanaz Rezaeian, Yousef Bozorgnia, I. M. Idriss, Kenneth Campbell, Norman Abrahamson, and Walter Silva. July 2012.

PEER 2011/10 *Earthquake Engineering for Resilient Communities: 2011 PEER Internship Program Research Report Collection.* Eds. Heidi Faison and Stephen A. Mahin. December 2011.

PEER 2011/09 *Calibration of Semi-Stochastic Procedure for Simulating High-Frequency Ground Motions.* Jonathan P. Stewart, Emel Seyhan, and Robert W. Graves. December 2011.

PEER 2011/08 *Water Supply in regard to Fire Following Earthquake.* Charles Scawthorn. November 2011.

PEER 2011/07 *Seismic Risk Management in Urban Areas. Proceedings of a U.S.-Iran-Turkey Seismic Workshop.* September 2011.

PEER 2011/06 *The Use of Base Isolation Systems to Achieve Complex Seismic Performance Objectives.* Troy A. Morgan and Stephen A. Mahin. July 2011.

PEER 2011/05 *Case Studies of the Seismic Performance of Tall Buildings Designed by Alternative Means.* Task 12 Report for the Tall Buildings Initiative. Jack Moehle, Yousef Bozorgnia, Nirmal Jayaram, Pierson Jones, Mohsen Rahnama, Nilesh Shome, Zeynep Tuna, John Wallace, Tony Yang, and Farzin Zareian. July 2011.

PEER 2011/04 *Recommended Design Practice for Pile Foundations in Laterally Spreading Ground.* Scott A. Ashford, Ross W. Boulanger, and Scott J. Brandenberg. June 2011.

PEER 2011/03 *New Ground Motion Selection Procedures and Selected Motions for the PEER Transportation Research Program.* Jack W. Baker, Ting Lin, Shrey K. Shahi, and Nirmal Jayaram. March 2011.

PEER 2011/02 *A Bayesian Network Methodology for Infrastructure Seismic Risk Assessment and Decision Support.* Michelle T. Bensi, Armen Der Kiureghian, and Daniel Straub. March 2011.

PEER 2011/01 *Demand Fragility Surfaces for Bridges in Liquefied and Laterally Spreading Ground.* Scott J. Brandenberg, Jian Zhang, Pirooz Kashighandi, Yili Huo, and Minxing Zhao. March 2011.

PEER 2010/05 *Guidelines for Performance-Based Seismic Design of Tall Buildings.* Developed by the Tall Buildings Initiative. November 2010.

PEER 2010/04 *Application Guide for the Design of Flexible and Rigid Bus Connections between Substation Equipment Subjected to Earthquakes.* Jean-Bernard Dastous and Armen Der Kiureghian. September 2010.

PEER 2010/03 *Shear Wave Velocity as a Statistical Function of Standard Penetration Test Resistance and Vertical Effective Stress at Caltrans Bridge Sites.* Scott J. Brandenberg, Naresh Bellana, and Thomas Shantz. June 2010.

PEER 2010/02 *Stochastic Modeling and Simulation of Ground Motions for Performance-Based Earthquake Engineering.* Sanaz Rezaeian and Armen Der Kiureghian. June 2010.

PEER 2010/01 *Structural Response and Cost Characterization of Bridge Construction Using Seismic Performance Enhancement Strategies.* Ady Aviram, Božidar Stojadinović, Gustavo J. Parra-Montesinos, and Kevin R. Mackie. March 2010.

PEER 2009/03 *The Integration of Experimental and Simulation Data in the Study of Reinforced Concrete Bridge Systems Including Soil-Foundation-Structure Interaction.* Matthew Dryden and Gregory L. Fenves. November 2009.

PEER 2009/02 *Improving Earthquake Mitigation through Innovations and Applications in Seismic Science, Engineering, Communication, and Response. Proceedings of a U.S.-Iran Seismic Workshop.* October 2009.

PEER 2009/01 *Evaluation of Ground Motion Selection and Modification Methods: Predicting Median Interstory Drift Response of Buildings.* Curt B. Haselton, Ed. June 2009.

PEER 2008/10 *Technical Manual for Strata.* Albert R. Kottke and Ellen M. Rathje. February 2009.

PEER 2008/09 *NGA Model for Average Horizontal Component of Peak Ground Motion and Response Spectra.* Brian S.-J. Chiou and Robert R. Youngs. November 2008.

PEER 2008/08 *Toward Earthquake-Resistant Design of Concentrically Braced Steel Structures.* Patxi Uriz and Stephen A. Mahin. November 2008.

PEER 2008/07 *Using OpenSees for Performance-Based Evaluation of Bridges on Liquefiable Soils.* Stephen L. Kramer, Pedro Arduino, and HyungSuk Shin. November 2008.

PEER 2008/06 *Shaking Table Tests and Numerical Investigation of Self-Centering Reinforced Concrete Bridge Columns.* Hyung IL Jeong, Junichi Sakai, and Stephen A. Mahin. September 2008.

PEER 2008/05 *Performance-Based Earthquake Engineering Design Evaluation Procedure for Bridge Foundations Undergoing Liquefaction-Induced Lateral Ground Displacement.* Christian A. Ledezma and Jonathan D. Bray. August 2008.

PEER 2008/04 *Benchmarking of Nonlinear Geotechnical Ground Response Analysis Procedures.* Jonathan P. Stewart, Annie On-Lei Kwok, Yousseff M. A. Hashash, Neven Matasovic, Robert Pyke, Zhiliang Wang, and Zhaohui Yang. August 2008.

PEER 2008/03 *Guidelines for Nonlinear Analysis of Bridge Structures in California.* Ady Aviram, Kevin R. Mackie, and Božidar Stojadinović. August 2008.

PEER 2008/02 *Treatment of Uncertainties in Seismic-Risk Analysis of Transportation Systems.* Evangelos Stergiou and Anne S. Kiremidjian. July 2008.

PEER 2008/01 *Seismic Performance Objectives for Tall Buildings.* William T. Holmes, Charles Kircher, William Petak, and Nabih Youssef. August 2008.

PEER 2007/12 *An Assessment to Benchmark the Seismic Performance of a Code-Conforming Reinforced Concrete Moment-Frame Building.* Curt Haselton, Christine A. Goulet, Judith Mitrani-Reiser, James L. Beck, Gregory G. Deierlein, Keith A. Porter, Jonathan P. Stewart, and Ertugrul Taciroglu. August 2008.

PEER 2007/11 *Bar Buckling in Reinforced Concrete Bridge Columns.* Wayne A. Brown, Dawn E. Lehman, and John F. Stanton. February 2008.

PEER 2007/10 *Computational Modeling of Progressive Collapse in Reinforced Concrete Frame Structures.* Mohamed M. Talaat and Khalid M. Mosalam. May 2008.

PEER 2007/09 *Integrated Probabilistic Performance-Based Evaluation of Benchmark Reinforced Concrete Bridges.* Kevin R. Mackie, John-Michael Wong, and Božidar Stojadinović. January 2008.

PEER 2007/08 *Assessing Seismic Collapse Safety of Modern Reinforced Concrete Moment-Frame Buildings.* Curt B. Haselton and Gregory G. Deierlein. February 2008.

PEER 2007/07 *Performance Modeling Strategies for Modern Reinforced Concrete Bridge Columns.* Michael P. Berry and Marc O. Eberhard. April 2008.

PEER 2007/06 *Development of Improved Procedures for Seismic Design of Buried and Partially Buried Structures.* Linda Al Atik and Nicholas Sitar. June 2007.

PEER 2007/05 *Uncertainty and Correlation in Seismic Risk Assessment of Transportation Systems.* Renee G. Lee and Anne S. Kiremidjian. July 2007.

PEER 2007/04 *Numerical Models for Analysis and Performance-Based Design of Shallow Foundations Subjected to Seismic Loading.* Sivapalan Gajan, Tara C. Hutchinson, Bruce L. Kutter, Prishati Raychowdhury, José A. Ugalde, and Jonathan P. Stewart. May 2008.

PEER 2007/03 *Beam-Column Element Model Calibrated for Predicting Flexural Response Leading to Global Collapse of RC Frame Buildings.* Curt B. Haselton, Abbie B. Liel, Sarah Taylor Lange, and Gregory G. Deierlein. May 2008.

PEER 2007/02 *Campbell-Bozorgnia NGA Ground Motion Relations for the Geometric Mean Horizontal Component of Peak and Spectral Ground Motion Parameters.* Kenneth W. Campbell and Yousef Bozorgnia. May 2007.

PEER 2007/01 *Boore-Atkinson NGA Ground Motion Relations for the Geometric Mean Horizontal Component of Peak and Spectral Ground Motion Parameters.* David M. Boore and Gail M. Atkinson. May. May 2007.

PEER 2006/12 *Societal Implications of Performance-Based Earthquake Engineering.* Peter J. May. May 2007.

PEER 2006/11 *Probabilistic Seismic Demand Analysis Using Advanced Ground Motion Intensity Measures, Attenuation Relationships, and Near-Fault Effects.* Polsak Tothong and C. Allin Cornell. March 2007.

PEER 2006/10 *Application of the PEER PBEE Methodology to the I-880 Viaduct.* Sashi Kunnath. February 2007.

PEER 2006/09 *Quantifying Economic Losses from Travel Forgone Following a Large Metropolitan Earthquake.* James Moore, Sungbin Cho, Yue Yue Fan, and Stuart Werner. November 2006.

PEER 2006/08 *Vector-Valued Ground Motion Intensity Measures for Probabilistic Seismic Demand Analysis.* Jack W. Baker and C. Allin Cornell. October 2006.

PEER 2006/07 *Analytical Modeling of Reinforced Concrete Walls for Predicting Flexural and Coupled–Shear-Flexural Responses.* Kutay Orakcal, Leonardo M. Massone, and John W. Wallace. October 2006.

PEER 2006/06 *Nonlinear Analysis of a Soil-Drilled Pier System under Static and Dynamic Axial Loading.* Gang Wang and Nicholas Sitar. November 2006.

PEER 2006/05 *Advanced Seismic Assessment Guidelines.* Paolo Bazzurro, C. Allin Cornell, Charles Menun, Maziar Motahari, and Nicolas Luco. September 2006.

PEER 2006/04 *Probabilistic Seismic Evaluation of Reinforced Concrete Structural Components and Systems.* Tae Hyung Lee and Khalid M. Mosalam. August 2006.

PEER 2006/03 *Performance of Lifelines Subjected to Lateral Spreading.* Scott A. Ashford and Teerawut Juirnarongrit. July 2006.

PEER 2006/02 *Pacific Earthquake Engineering Research Center Highway Demonstration Project.* Anne Kiremidjian, James Moore, Yue Yue Fan, Nesrin Basoz, Ozgur Yazali, and Meredith Williams. April 2006.

PEER 2006/01 *Bracing Berkeley. A Guide to Seismic Safety on the UC Berkeley Campus.* Mary C. Comerio, Stephen Tobriner, and Ariane Fehrenkamp. January 2006.

PEER 2005/16 *Seismic Response and Reliability of Electrical Substation Equipment and Systems.* Junho Song, Armen Der Kiureghian, and Jerome L. Sackman. April 2006.

PEER 2005/15 *CPT-Based Probabilistic Assessment of Seismic Soil Liquefaction Initiation.* R. E. S. Moss, R. B. Seed, R. E. Kayen, J. P. Stewart, and A. Der Kiureghian. April 2006.

PEER 2005/14 *Workshop on Modeling of Nonlinear Cyclic Load-Deformation Behavior of Shallow Foundations.* Bruce L. Kutter, Geoffrey Martin, Tara Hutchinson, Chad Harden, Sivapalan Gajan, and Justin Phalen. March 2006.

PEER 2005/13 *Stochastic Characterization and Decision Bases under Time-Dependent Aftershock Risk in Performance-Based Earthquake Engineering.* Gee Liek Yeo and C. Allin Cornell. July 2005.

PEER 2005/12 *PEER Testbed Study on a Laboratory Building: Exercising Seismic Performance Assessment.* Mary C. Comerio, editor. November 2005.

PEER 2005/11 *Van Nuys Hotel Building Testbed Report: Exercising Seismic Performance Assessment.* Helmut Krawinkler, editor. October 2005.

PEER 2005/10 *First NEES/E-Defense Workshop on Collapse Simulation of Reinforced Concrete Building Structures.* September 2005.

PEER 2005/09 *Test Applications of Advanced Seismic Assessment Guidelines.* Joe Maffei, Karl Telleen, Danya Mohr, William Holmes, and Yuki Nakayama. August 2006.

PEER 2005/08 *Damage Accumulation in Lightly Confined Reinforced Concrete Bridge Columns.* R. Tyler Ranf, Jared M. Nelson, Zach Price, Marc O. Eberhard, and John F. Stanton. April 2006.

PEER 2005/07 *Experimental and Analytical Studies on the Seismic Response of Freestanding and Anchored Laboratory Equipment.* Dimitrios Konstantinidis and Nicos Makris. January 2005.

PEER 2005/06 *Global Collapse of Frame Structures under Seismic Excitations.* Luis F. Ibarra and Helmut Krawinkler. September 2005.

PEER 2005//05 *Performance Characterization of Bench- and Shelf-Mounted Equipment.* Samit Ray Chaudhuri and Tara C. Hutchinson. May 2006.

PEER 2005/04 *Numerical Modeling of the Nonlinear Cyclic Response of Shallow Foundations.* Chad Harden, Tara Hutchinson, Geoffrey R. Martin, and Bruce L. Kutter. August 2005.

PEER 2005/03 *A Taxonomy of Building Components for Performance-Based Earthquake Engineering.* Keith A. Porter. September 2005.

PEER 2005/02 *Fragility Basis for California Highway Overpass Bridge Seismic Decision Making.* Kevin R. Mackie and Božidar Stojadinović. June 2005.

PEER 2005/01 *Empirical Characterization of Site Conditions on Strong Ground Motion.* Jonathan P. Stewart, Yoojoong Choi, and Robert W. Graves. June 2005.

PEER 2004/09 *Electrical Substation Equipment Interaction: Experimental Rigid Conductor Studies.* Christopher Stearns and André Filiatrault. February 2005.

PEER 2004/08 *Seismic Qualification and Fragility Testing of Line Break 550-kV Disconnect Switches.* Shakhzod M. Takhirov, Gregory L. Fenves, and Eric Fujisaki. January 2005.

PEER 2004/07 *Ground Motions for Earthquake Simulator Qualification of Electrical Substation Equipment.* Shakhzod M. Takhirov, Gregory L. Fenves, Eric Fujisaki, and Don Clyde. January 2005.

PEER 2004/06 *Performance-Based Regulation and Regulatory Regimes.* Peter J. May and Chris Koski. September 2004.

PEER 2004/05 *Performance-Based Seismic Design Concepts and Implementation: Proceedings of an International Workshop.* Peter Fajfar and Helmut Krawinkler, editors. September 2004.

PEER 2004/04 *Seismic Performance of an Instrumented Tilt-up Wall Building.* James C. Anderson and Vitelmo V. Bertero. July 2004.

PEER 2004/03 *Evaluation and Application of Concrete Tilt-up Assessment Methodologies.* Timothy Graf and James O. Malley. October 2004.

PEER 2004/02 *Analytical Investigations of New Methods for Reducing Residual Displacements of Reinforced Concrete Bridge Columns.* Junichi Sakai and Stephen A. Mahin. August 2004.

PEER 2004/01 *Seismic Performance of Masonry Buildings and Design Implications.* Kerri Anne Taeko Tokoro, James C. Anderson, and Vitelmo V. Bertero. February 2004.

PEER 2003/18 *Performance Models for Flexural Damage in Reinforced Concrete Columns.* Michael Berry and Marc Eberhard. August 2003.

PEER 2003/17 *Predicting Earthquake Damage in Older Reinforced Concrete Beam-Column Joints.* Catherine Pagni and Laura Lowes. October 2004.

PEER 2003/16 *Seismic Demands for Performance-Based Design of Bridges.* Kevin Mackie and Božidar Stojadinović. August 2003.

PEER 2003/15 *Seismic Demands for Nondeteriorating Frame Structures and Their Dependence on Ground Motions.* Ricardo Antonio Medina and Helmut Krawinkler. May 2004.

PEER 2003/14 *Finite Element Reliability and Sensitivity Methods for Performance-Based Earthquake Engineering.* Terje Haukaas and Armen Der Kiureghian. April 2004.

PEER 2003/13 *Effects of Connection Hysteretic Degradation on the Seismic Behavior of Steel Moment-Resisting Frames.* Janise E. Rodgers and Stephen A. Mahin. March 2004.

PEER 2003/12 *Implementation Manual for the Seismic Protection of Laboratory Contents: Format and Case Studies.* William T. Holmes and Mary C. Comerio. October 2003.

PEER 2003/11 *Fifth U.S.-Japan Workshop on Performance-Based Earthquake Engineering Methodology for Reinforced Concrete Building Structures.* February 2004.

PEER 2003/10 *A Beam-Column Joint Model for Simulating the Earthquake Response of Reinforced Concrete Frames.* Laura N. Lowes, Nilanjan Mitra, and Arash Altoontash. February 2004.

PEER 2003/09 *Sequencing Repairs after an Earthquake: An Economic Approach.* Marco Casari and Simon J. Wilkie. April 2004.

PEER 2003/08 *A Technical Framework for Probability-Based Demand and Capacity Factor Design (DCFD) Seismic Formats*. Fatemeh Jalayer and C. Allin Cornell. November 2003.

PEER 2003/07 *Uncertainty Specification and Propagation for Loss Estimation Using FOSM Methods.* Jack W. Baker and C. Allin Cornell. September 2003.

PEER 2003/06 *Performance of Circular Reinforced Concrete Bridge Columns under Bidirectional Earthquake Loading*. Mahmoud M. Hachem, Stephen A. Mahin, and Jack P. Moehle. February 2003.

PEER 2003/05 *Response Assessment for Building-Specific Loss Estimation.* Eduardo Miranda and Shahram Taghavi. September 2003.

PEER 2003/04 *Experimental Assessment of Columns with Short Lap Splices Subjected to Cyclic Loads*. Murat Melek, John W. Wallace, and Joel Conte. April 2003.

PEER 2003/03 *Probabilistic Response Assessment for Building-Specific Loss Estimation.* Eduardo Miranda and Hesameddin Aslani. September 2003.

PEER 2003/02 *Software Framework for Collaborative Development of Nonlinear Dynamic Analysis Program.* Jun Peng and Kincho H. Law. September 2003.

PEER 2003/01 *Shake Table Tests and Analytical Studies on the Gravity Load Collapse of Reinforced Concrete Frames.* Kenneth John Elwood and Jack P. Moehle. November 2003.

PEER 2002/24 *Performance of Beam to Column Bridge Joints Subjected to a Large Velocity Pulse.* Natalie Gibson, André Filiatrault, and Scott A. Ashford. April 2002.

PEER 2002/23 *Effects of Large Velocity Pulses on Reinforced Concrete Bridge Columns.* Greg L. Orozco and Scott A. Ashford. April 2002.

PEER 2002/22 *Characterization of Large Velocity Pulses for Laboratory Testing.* Kenneth E. Cox and Scott A. Ashford. April 2002.

PEER 2002/21 *Fourth U.S.-Japan Workshop on Performance-Based Earthquake Engineering Methodology for Reinforced Concrete Building Structures*. December 2002.

PEER 2002/20 *Barriers to Adoption and Implementation of PBEE Innovations.* Peter J. May. August 2002.

PEER 2002/19 *Economic-Engineered Integrated Models for Earthquakes: Socioeconomic Impacts.* Peter Gordon, James E. Moore II, and Harry W. Richardson. July 2002.

PEER 2002/18 *Assessment of Reinforced Concrete Building Exterior Joints with Substandard Details.* Chris P. Pantelides, Jon Hansen, Justin Nadauld, and Lawrence D. Reaveley. May 2002.

PEER 2002/17 *Structural Characterization and Seismic Response Analysis of a Highway Overcrossing Equipped with Elastomeric Bearings and Fluid Dampers: A Case Study.* Nicos Makris and Jian Zhang. November 2002.

PEER 2002/16 *Estimation of Uncertainty in Geotechnical Properties for Performance-Based Earthquake Engineering.* Allen L. Jones, Steven L. Kramer, and Pedro Arduino. December 2002.

PEER 2002/15 *Seismic Behavior of Bridge Columns Subjected to Various Loading Patterns.* Asadollah Esmaeily-Gh. and Yan Xiao. December 2002.

PEER 2002/14 *Inelastic Seismic Response of Extended Pile Shaft Supported Bridge Structures.* T.C. Hutchinson, R.W. Boulanger, Y.H. Chai, and I.M. Idriss. December 2002.

PEER 2002/13 *Probabilistic Models and Fragility Estimates for Bridge Components and Systems.* Paolo Gardoni, Armen Der Kiureghian, and Khalid M. Mosalam. June 2002.

PEER 2002/12 *Effects of Fault Dip and Slip Rake on Near-Source Ground Motions: Why Chi-Chi Was a Relatively Mild M7.6 Earthquake.* Brad T. Aagaard, John F. Hall, and Thomas H. Heaton. December 2002.

PEER 2002/11 *Analytical and Experimental Study of Fiber-Reinforced Strip Isolators*. James M. Kelly and Shakhzod M. Takhirov. September 2002.

PEER 2002/10 *Centrifuge Modeling of Settlement and Lateral Spreading with Comparisons to Numerical Analyses***.** Sivapalan Gajan and Bruce L. Kutter. January 2003.

PEER 2002/09 *Documentation and Analysis of Field Case Histories of Seismic Compression during the 1994 Northridge, California, Earthquake.* Jonathan P. Stewart, Patrick M. Smith, Daniel H. Whang, and Jonathan D. Bray. October 2002.

PEER 2002/08 *Component Testing, Stability Analysis and Characterization of Buckling-Restrained Unbonded Braces™.* Cameron Black, Nicos Makris, and Ian Aiken. September 2002.

PEER 2002/07 *Seismic Performance of Pile-Wharf Connections.* Charles W. Roeder, Robert Graff, Jennifer Soderstrom, and Jun Han Yoo. December 2001.

PEER 2002/06 *The Use of Benefit-Cost Analysis for Evaluation of Performance-Based Earthquake Engineering Decisions*. Richard O. Zerbe and Anthony Falit-Baiamonte. September 2001.

PEER 2002/05 *Guidelines, Specifications, and Seismic Performance Characterization of Nonstructural Building Components and Equipment*. André Filiatrault, Constantin Christopoulos, and Christopher Stearns. September 2001.

PEER 2002/04 *Consortium of Organizations for Strong-Motion Observation Systems and the Pacific Earthquake Engineering Research Center Lifelines Program: Invited Workshop on Archiving and Web Dissemination of Geotechnical Data, 4–5 October 2001*. September 2002.

PEER 2002/03 *Investigation of Sensitivity of Building Loss Estimates to Major Uncertain Variables for the Van Nuys Testbed.* Keith A. Porter, James L. Beck, and Rustem V. Shaikhutdinov. August 2002.

PEER 2002/02 *The Third U.S.-Japan Workshop on Performance-Based Earthquake Engineering Methodology for Reinforced Concrete Building Structures*. July 2002.

PEER 2002/01 *Nonstructural Loss Estimation: The UC Berkeley Case Study.* Mary C. Comerio and John C. Stallmeyer. December 2001.

PEER 2001/16 *Statistics of SDF-System Estimate of Roof Displacement for Pushover Analysis of Buildings.* Anil K. Chopra, Rakesh K. Goel, and Chatpan Chintanapakdee. December 2001.

PEER 2001/15 *Damage to Bridges during the 2001 Nisqually Earthquake.* R. Tyler Ranf, Marc O. Eberhard, and Michael P. Berry. November 2001.

PEER 2001/14 *Rocking Response of Equipment Anchored to a Base Foundation.* Nicos Makris and Cameron J. Black. September 2001.

PEER 2001/13 *Modeling Soil Liquefaction Hazards for Performance-Based Earthquake Engineering.* Steven L. Kramer and Ahmed-W. Elgamal. February 2001.

PEER 2001/12 *Development of Geotechnical Capabilities in OpenSees.* Boris Jeremić. September 2001.

PEER 2001/11 *Analytical and Experimental Study of Fiber-Reinforced Elastomeric Isolators*. James M. Kelly and Shakhzod M. Takhirov. September 2001.

PEER 2001/10 *Amplification Factors for Spectral Acceleration in Active Regions.* Jonathan P. Stewart, Andrew H. Liu, Yoojoong Choi, and Mehmet B. Baturay. December 2001.

PEER 2001/09 *Ground Motion Evaluation Procedures for Performance-Based Design.* Jonathan P. Stewart, Shyh-Jeng Chiou, Jonathan D. Bray, Robert W. Graves, Paul G. Somerville, and Norman A. Abrahamson. September 2001.

PEER 2001/08 *Experimental and Computational Evaluation of Reinforced Concrete Bridge Beam-Column Connections for Seismic Performance*. Clay J. Naito, Jack P. Moehle, and Khalid M. Mosalam. November 2001.

PEER 2001/07 *The Rocking Spectrum and the Shortcomings of Design Guidelines.* Nicos Makris and Dimitrios Konstantinidis. August 2001.

PEER 2001/06 *Development of an Electrical Substation Equipment Performance Database for Evaluation of Equipment Fragilities*. Thalia Agnanos. April 1999.

PEER 2001/05 *Stiffness Analysis of Fiber-Reinforced Elastomeric Isolators.* Hsiang-Chuan Tsai and James M. Kelly. May 2001.

PEER 2001/04 *Organizational and Societal Considerations for Performance-Based Earthquake Engineering.* Peter J. May. April 2001.

PEER 2001/03 *A Modal Pushover Analysis Procedure to Estimate Seismic Demands for Buildings: Theory and Preliminary Evaluation.* Anil K. Chopra and Rakesh K. Goel. January 2001.

PEER 2001/02 *Seismic Response Analysis of Highway Overcrossings Including Soil-Structure Interaction.* Jian Zhang and Nicos Makris. March 2001.

PEER 2001/01 *Experimental Study of Large Seismic Steel Beam-to-Column Connections.* Egor P. Popov and Shakhzod M. Takhirov. November 2000.

PEER 2000/10 *The Second U.S.-Japan Workshop on Performance-Based Earthquake Engineering Methodology for Reinforced Concrete Building Structures.* March 2000.

PEER 2000/09 *Structural Engineering Reconnaissance of the August 17, 1999 Earthquake: Kocaeli (Izmit), Turkey*. Halil Sezen, Kenneth J. Elwood, Andrew S. Whittaker, Khalid Mosalam, John J. Wallace, and John F. Stanton. December 2000.

PEER 2000/08 *Behavior of Reinforced Concrete Bridge Columns Having Varying Aspect Ratios and Varying Lengths of Confinement.* Anthony J. Calderone, Dawn E. Lehman, and Jack P. Moehle. January 2001.

PEER 2000/07 *Cover-Plate and Flange-Plate Reinforced Steel Moment-Resisting Connections.* Taejin Kim, Andrew S. Whittaker, Amir S. Gilani, Vitelmo V. Bertero, and Shakhzod M. Takhirov. September 2000.

PEER 2000/06 *Seismic Evaluation and Analysis of 230-kV Disconnect Switches.* Amir S. J. Gilani, Andrew S. Whittaker, Gregory L. Fenves, Chun-Hao Chen, Henry Ho, and Eric Fujisaki. July 2000.

PEER 2000/05 *Performance-Based Evaluation of Exterior Reinforced Concrete Building Joints for Seismic Excitation.* Chandra Clyde, Chris P. Pantelides, and Lawrence D. Reaveley. July 2000.

PEER 2000/04 *An Evaluation of Seismic Energy Demand: An Attenuation Approach.* Chung-Che Chou and Chia-Ming Uang. July 1999.

PEER 2000/03 *Framing Earthquake Retrofitting Decisions: The Case of Hillside Homes in Los Angeles.* Detlof von Winterfeldt, Nels Roselund, and Alicia Kitsuse. March 2000.

PEER 2000/02 *U.S.-Japan Workshop on the Effects of Near-Field Earthquake Shaking.* Andrew Whittaker, ed. July 2000.

PEER 2000/01 *Further Studies on Seismic Interaction in Interconnected Electrical Substation Equipment.* Armen Der Kiureghian, Kee-Jeung Hong, and Jerome L. Sackman. November 1999.

PEER 1999/14 *Seismic Evaluation and Retrofit of 230-kV Porcelain Transformer Bushings.* Amir S. Gilani, Andrew S. Whittaker, Gregory L. Fenves, and Eric Fujisaki. December 1999.

PEER 1999/13 *Building Vulnerability Studies: Modeling and Evaluation of Tilt-up and Steel Reinforced Concrete Buildings.* John W. Wallace, Jonathan P. Stewart, and Andrew S. Whittaker, editors. December 1999.

PEER 1999/12 *Rehabilitation of Nonductile RC Frame Building Using Encasement Plates and Energy-Dissipating Devices.* Mehrdad Sasani, Vitelmo V. Bertero, James C. Anderson. December 1999.

PEER 1999/11 *Performance Evaluation Database for Concrete Bridge Components and Systems under Simulated Seismic Loads.* Yael D. Hose and Frieder Seible. November 1999.

PEER 1999/10 *U.S.-Japan Workshop on Performance-Based Earthquake Engineering Methodology for Reinforced Concrete Building Structures.* December 1999.

PEER 1999/09 *Performance Improvement of Long Period Building Structures Subjected to Severe Pulse-Type Ground Motions*. James C. Anderson, Vitelmo V. Bertero, and Raul Bertero. October 1999.

PEER 1999/08 *Envelopes for Seismic Response Vectors.* Charles Menun and Armen Der Kiureghian. July 1999.

PEER 1999/07 *Documentation of Strengths and Weaknesses of Current Computer Analysis Methods for Seismic Performance of Reinforced Concrete Members.* William F. Cofer. November 1999.

PEER 1999/06 *Rocking Response and Overturning of Anchored Equipment under Seismic Excitations.* Nicos Makris and Jian Zhang. November 1999.

PEER 1999/05 *Seismic Evaluation of 550 kV Porcelain Transformer Bushings.* Amir S. Gilani, Andrew S. Whittaker, Gregory L. Fenves, and Eric Fujisaki. October 1999.

PEER 1999/04 *Adoption and Enforcement of Earthquake Risk-Reduction Measures.* Peter J. May, Raymond J. Burby, T. Jens Feeley, and Robert Wood.

PEER 1999/03 *Task 3 Characterization of Site Response General Site Categories*. Adrian Rodriguez-Marek, Jonathan D. Bray, and Norman Abrahamson. February 1999.

PEER 1999/02 *Capacity-Demand-Diagram Methods for Estimating Seismic Deformation of Inelastic Structures: SDF Systems*. Anil K. Chopra and Rakesh Goel. April 1999.

PEER 1999/01 *Interaction in Interconnected Electrical Substation Equipment Subjected to Earthquake Ground Motions.* Armen Der Kiureghian, Jerome L. Sackman, and Kee-Jeung Hong. February 1999.

PEER 1998/08 *Behavior and Failure Analysis of a Multiple-Frame Highway Bridge in the 1994 Northridge Earthquake.* Gregory L. Fenves and Michael Ellery. December 1998.

PEER 1998/07 *Empirical Evaluation of Inertial Soil-Structure Interaction Effects.* Jonathan P. Stewart, Raymond B. Seed, and Gregory L. Fenves. November 1998.

PEER 1998/06 *Effect of Damping Mechanisms on the Response of Seismic Isolated Structures.* Nicos Makris and Shih-Po Chang. November 1998.

PEER 1998/05 *Rocking Response and Overturning of Equipment under Horizontal Pulse-Type Motions.* Nicos Makris and Yiannis Roussos. October 1998.

PEER 1998/04 *Pacific Earthquake Engineering Research Invitational Workshop Proceedings, May 14–15, 1998: Defining the Links between Planning, Policy Analysis, Economics and Earthquake Engineering.* Mary Comerio and Peter Gordon. September 1998.

PEER 1998/03 *Repair/Upgrade Procedures for Welded Beam to Column Connections.* James C. Anderson and Xiaojing Duan. May 1998.

PEER 1998/02 *Seismic Evaluation of 196 kV Porcelain Transformer Bushings.* Amir S. Gilani, Juan W. Chavez, Gregory L. Fenves, and Andrew S. Whittaker. May 1998.

PEER 1998/01 *Seismic Performance of Well-Confined Concrete Bridge Columns.* Dawn E. Lehman and Jack P. Moehle. December 2000.

ONLINE PEER REPORTS

The following PEER reports are available by Internet only at http://peer.berkeley.edu/publications/peer_reports_complete.html.

PEER 2012/103 *Performance-Based Seismic Demand Assessment of Concentrically Braced Steel Frame Buildings.* Chui-Hsin Chen and Stephen A. Mahin. December 2012.

PEER 2012/102 *Procedure to Restart an Interrupted Hybrid Simulation: Addendum to PEER Report 2010/103.* Vesna Terzic and Bozidar Stojadinovic. October 2012.

PEER 2012/101 *Mechanics of Fiber Reinforced Bearings.* James M. Kelly and Andrea Calabrese. February 2012.

PEER 2011/107 *Nonlinear Site Response and Seismic Compression at Vertical Array Strongly Shaken by 2007 Niigata-ken Chuetsu-oki Earthquake.* Eric Yee, Jonathan P. Stewart, and Kohji Tokimatsu. December 2011.

PEER 2011/106 *Self Compacting Hybrid Fiber Reinforced Concrete Composites for Bridge Columns.* Pardeep Kumar, Gabriel Jen, William Trono, Marios Panagiotou, and Claudia Ostertag. September 2011.

PEER 2011/105 *Stochastic Dynamic Analysis of Bridges Subjected to Spacially Varying Ground Motions.* Katerina Konakli and Armen Der Kiureghian. August 2011.

PEER 2011/104 *Design and Instrumentation of the 2010 E-Defense Four-Story Reinforced Concrete and Post-Tensioned Concrete Buildings.* Takuya Nagae, Kenichi Tahara, Taizo Matsumori, Hitoshi Shiohara, Toshimi Kabeyasawa, Susumu Kono, Minehiro Nishiyama (Japanese Research Team) and John Wallace, Wassim Ghannoum, Jack Moehle, Richard Sause, Wesley Keller, Zeynep Tuna (U.S. Research Team). June 2011.

PEER 2011/103 *In-Situ Monitoring of the Force Output of Fluid Dampers: Experimental Investigation.* Dimitrios Konstantinidis, James M. Kelly, and Nicos Makris. April 2011.

PEER 2011/102 *Ground-motion prediction equations 1964 - 2010.* John Douglas. April 2011.

PEER 2011/101 *Report of the Eighth Planning Meeting of NEES/E-Defense Collaborative Research on Earthquake Engineering.* Convened by the Hyogo Earthquake Engineering Research Center (NIED), NEES Consortium, Inc. February 2011.

PEER 2010/111 *Modeling and Acceptance Criteria for Seismic Design and Analysis of Tall Buildings.* Task 7 Report for the Tall Buildings Initiative - Published jointly by the Applied Technology Council. October 2010.

PEER 2010/110 *Seismic Performance Assessment and Probabilistic Repair Cost Analysis of Precast Concrete Cladding Systems for Multistory Buildlings.* Jeffrey P. Hunt and Božidar Stojadinovic. November 2010.

PEER 2010/109 *Report of the Seventh Joint Planning Meeting of NEES/E-Defense Collaboration on Earthquake Engineering. Held at the E-Defense, Miki, and Shin-Kobe, Japan, September 18–19, 2009.* August 2010.

PEER 2010/108 *Probabilistic Tsunami Hazard in California.* Hong Kie Thio, Paul Somerville, and Jascha Polet, preparers. October 2010.

PEER 2010/107 *Performance and Reliability of Exposed Column Base Plate Connections for Steel Moment-Resisting Frames.* Ady Aviram, Božidar Stojadinovic, and Armen Der Kiureghian. August 2010.

PEER 2010/106 *Verification of Probabilistic Seismic Hazard Analysis Computer Programs.* Patricia Thomas, Ivan Wong, and Norman Abrahamson. May 2010.

PEER 2010/105 *Structural Engineering Reconnaissance of the April 6, 2009, Abruzzo, Italy, Earthquake, and Lessons Learned.* M. Selim Günay and Khalid M. Mosalam. April 2010.

PEER 2010/104 *Simulating the Inelastic Seismic Behavior of Steel Braced Frames, Including the Effects of Low-Cycle Fatigue.* Yuli Huang and Stephen A. Mahin. April 2010.

PEER 2010/103 *Post-Earthquake Traffic Capacity of Modern Bridges in California.* Vesna Terzic and Božidar Stojadinović. March 2010.

PEER 2010/102 *Analysis of Cumulative Absolute Velocity (CAV) and JMA Instrumental Seismic Intensity (I_{JMA}) Using the PEER–NGA Strong Motion Database.* Kenneth W. Campbell and Yousef Bozorgnia. February 2010.

PEER 2010/101 *Rocking Response of Bridges on Shallow Foundations.* Jose A. Ugalde, Bruce L. Kutter, and Boris Jeremic. April 2010.

PEER 2009/109 *Simulation and Performance-Based Earthquake Engineering Assessment of Self-Centering Post-Tensioned Concrete Bridge Systems.* Won K. Lee and Sarah L. Billington. December 2009.

PEER 2009/108 *PEER Lifelines Geotechnical Virtual Data Center.* J. Carl Stepp, Daniel J. Ponti, Loren L. Turner, Jennifer N. Swift, Sean Devlin, Yang Zhu, Jean Benoit, and John Bobbitt. September 2009.

PEER 2009/107 *Experimental and Computational Evaluation of Current and Innovative In-Span Hinge Details in Reinforced Concrete Box-Girder Bridges: Part 2: Post-Test Analysis and Design Recommendations.* Matias A. Hube and Khalid M. Mosalam. December 2009.

PEER 2009/106 *Shear Strength Models of Exterior Beam-Column Joints without Transverse Reinforcement.* Sangjoon Park and Khalid M. Mosalam. November 2009.

PEER 2009/105 *Reduced Uncertainty of Ground Motion Prediction Equations through Bayesian Variance Analysis.* Robb Eric S. Moss. November 2009.

PEER 2009/104 *Advanced Implementation of Hybrid Simulation.* Andreas H. Schellenberg, Stephen A. Mahin, Gregory L. Fenves. November 2009.

PEER 2009/103 *Performance Evaluation of Innovative Steel Braced Frames.* T. Y. Yang, Jack P. Moehle, and Božidar Stojadinovic. August 2009.

PEER 2009/102 *Reinvestigation of Liquefaction and Nonliquefaction Case Histories from the 1976 Tangshan Earthquake.* Robb Eric Moss, Robert E. Kayen, Liyuan Tong, Songyu Liu, Guojun Cai, and Jiaer Wu. August 2009.

PEER 2009/101 *Report of the First Joint Planning Meeting for the Second Phase of NEES/E-Defense Collaborative Research on Earthquake Engineering.* Stephen A. Mahin et al. July 2009.

PEER 2008/104 *Experimental and Analytical Study of the Seismic Performance of Retaining Structures.* Linda Al Atik and Nicholas Sitar. January 2009.

PEER 2008/103 *Experimental and Computational Evaluation of Current and Innovative In-Span Hinge Details in Reinforced Concrete Box-Girder Bridges. Part 1: Experimental Findings and Pre-Test Analysis.* Matias A. Hube and Khalid M. Mosalam. January 2009.

PEER 2008/102 *Modeling of Unreinforced Masonry Infill Walls Considering In-Plane and Out-of-Plane Interaction.* Stephen Kadysiewski and Khalid M. Mosalam. January 2009.

PEER 2008/101 *Seismic Performance Objectives for Tall Buildings.* William T. Holmes, Charles Kircher, William Petak, and Nabih Youssef. August 2008.

PEER 2007/101 *Generalized Hybrid Simulation Framework for Structural Systems Subjected to Seismic Loading.* Tarek Elkhoraibi and Khalid M. Mosalam. July 2007.

PEER 2007/100 *Seismic Evaluation of Reinforced Concrete Buildings Including Effects of Masonry Infill Walls.* Alidad Hashemi and Khalid M. Mosalam. July 2007.

The Pacific Earthquake Engineering Research Center (PEER) is a multi-institutional research and education center with headquarters at the University of California, Berkeley. Investigators from over 20 universities, several consulting companies, and researchers at various state and federal government agencies contribute to research programs focused on performance-based earthquake engineering.

These research programs aim to identify and reduce the risks from major earthquakes to life safety and to the economy by including research in a wide variety of disciplines including structural and geotechnical engineering, geology/seismology, lifelines, transportation, architecture, economics, risk management, and public policy.

PEER is supported by federal, state, local, and regional agencies, together with industry partners.

PEER Core Institutions:
University of California, Berkeley (Lead Institution)
California Institute of Technology
Oregon State University
Stanford University
University of California, Davis
University of California, Irvine
University of California, Los Angeles
University of California, San Diego
University of Southern California
University of Washington

PEER reports can be ordered at http://peer.berkeley.edu/publications/peer_reports.html or by contacting

Pacific Earthquake Engineering Research Center
University of California, Berkeley
325 Davis Hall, mail code 1792
Berkeley, CA 94720-1792
Tel: 510-642-3437
Fax: 510-642-1655
Email: peer_editor@berkeley.edu

ISSN 1547-0587X